Universidade de Aveiro Departamento de Electrónica, Telecomunicações e Informática,
2018

Alexandre Rui Reis Fontes

Técnicas de Teste de Circuitos Óticos Integrados para Redes PON

Test Techniques of Photonic Integrated Circuits for PON Networks

Universidade de Aveiro Departamento de Electrónica, Telecomunicações e Informática,
2018

Alexandre Rui Reis Fontes

Técnicas de Teste de Circuitos Óticos Integrados para Redes PON

Test Techniques of Photonic Integrated Circuits for PON Networks

Dissertação apresentada à Universidade de Aveiro para cumprimento dos requisitos necessários à obtenção do grau de Mestre em Engenharia Electrónica e Telecomunicações, realizada sob a orientação cientifica de Dr. Mário Lima, Professor do Departamento de Eletrónica, Telecomunicações e Informática da Univerdade de Aveiro, e co-orientação do Eng. Francisco Rodrigues da PICadvanced S.A.

Dedico este trabalho aos meus pais e aos meus irmãos.

o júri / the jury

presidente / president	**Professor Doutor José Rodrigues Ferreira da Rocha** Professor Catedrático da Universidade de Aveiro
vogais / examiners committee	**Professor Doutor Mário José Neves de Lima** Professor Auxiliar da Universidade de Aveiro (orientador)
	Professora Doutora Maria do Carmo Raposo Medeiros Professora Associada da Universidade de Coimbra

agradecimentos / acknowledgements

Este trabalho marca uma fase decisiva da minha vida académica, cujo sucesso resultou do contributo de várias pessoas que me apoiaram ao longo do percurso e às quais gostaria de prestar o meu humilde reconhecimento.

Queria começar por agradecer aos meus orientadores, ao Prof. Mário Lima pela disponibilidade em ajudar, pelo apoio constante, pelas sugestões e referências, pela paciência, pela recetividade e acolhimento, promovendo um ambiente excecional de trabalho, ao Prof. António Teixeira e ao Eng. Francisco Rodrigues, pelos ensinamentos, pelos conselhos e incentivos e também pela disponibilidade.

A minha gratidão e reconhecimento ao grupo de ótica do IT e ao pessoal da PICadvanced, em particular ao Hugo Neto, à Carla Rodrigues e à Ana Tavares, por toda a colaboração, pelos contributos e pela tolerância.

À Sandra Pereira e ao Bruno Barbosa pela excelente ajuda nesta fase final da minha etapa académica.

Um especial agradecimento a todos os meus amigos da Universidade de Aveiro por estes cinco anos inesquecíveis. A amizade, os agradáveis momentos que vivemos, o convívio social, a união e a compreensão foram os meus alicerces tanto a nível académico como a nível pessoal.

Aos meus amigos de Santa Maria, um enorme obrigado, pois, mesmo estando afastados geograficamente uns dos outros, foram pilares de apoio, de orientação e de motivação, demonstrando que a verdadeira amizade que nos une é fortalecida pela distância.

Por fim, mas mais importante, um GRANDE OBRIGADO, à minha familia toda em especial aos meus pais e meus irmãos que, mesmo estando longe, estiveram sempre tão perto. Por acreditarem sempre em mim com enorme orgulho, não me deixando desistir, pois nos momentos menos bons foram o meu consolo e ombro amigo. Por todos os conselhos e ensinamentos dados. OBRIGADO!

palavras-Chave Comunicações Óticas, PIC, Test Bench, Medições

Resumo

As comunicações óticas fazem parte do nosso dia a dia, pois atualmente são a base das infraestruturas de telecomunicações, destacando-se pela qualidade e eficiência na transmissão de dados. Devido ao desenvolvimento tecnológico que caracteriza o nosso quotidiano, torna-se necessário a evolução destas infraestruturas de comunicação para satisfazer as necessidades e exigências do consumidor final.

A Rede Ótica Passiva (PON) é uma das várias arquiteturas de distribuição de fibra ótica até ao consumidor final e caracteriza-se pelo baixo custo de implementação e de manutenção e pela divisão de banda larga disponível aos clientes. No entanto, e tendo em consideração o incremento do acesso à informação através dos canais digitais, impõe-se otimizar os custos dessa rede, aumentar a sua rapidez, ampliar a quantidade de informação e melhorar cada vez mais a qualidade da transmissão dos dados.

O recurso, no futuro, à utilização dos Circuitos Óticos Integrados (PIC) permitirá melhorar as redes PON, pois estes circuitos consistem em chips que integram vários componentes óticos capazes de ter variadíssimas funcionalidades. A caracterização e teste destes chips encontram-se ainda numa fase inicial e pouco otimizada nos nossos laboratórios.

Neste contexto, este trabalho consistiu na realização de testes que permitissem definir um protocolo de teste e apresentar uma proposta de um setup de teste genérico, sendo o principal objetivo desta dissertação que a mesma possa ser utilizada como ferramenta com todos os passos necessários à realização destes testes.

Inicialmente é feito um enquadramento teórico acerca de redes óticas passivas (PON) e de circuitos óticos integrados (PIC). De seguida, é apresentado um capítulo sobre teoria de medidas e o tratamento correto dos dados obtidos numa experiência. Depois são apresentados alguns testes de PICs realizados em laboratório, constatando-se as dificuldades dos mesmos. No fim, é proposto um setup de teste genérico, acompanhado de um protocolo de teste, tendo como objetivo a otimização do tempo gasto na experiência, e da qualidade da receção e tratamento dos dados recebidos.

Este trabalho foi efectuado no âmbito dos projetos COMPRESS - PTDC/EEI-TEL/7163/2014 e HEATIT 017942 (CENTRO-01-0247-FEDER-017942)

keywords Optical Communications, PIC, Test Bench, Measurements

Abstract

Optical communications are part of our daily routines being the basis of most of nowadays telecommunications infrastructures, standing out for the quality and efficiency concerning the data transmission. Thanks to the technological advances, there is a need to develop these communication infrastructures in order to satisfy the consumer's needs.

Passive Optical Network (PON) is one of the architectures used to bring optical fiber to the final consumer. Its implementation and conservation are inexpensive, and the bandwidth is divided by the connected users. However, with the increasing access to information through digital channels it is necessary to optimize costs, increase its rate, widen the amount of information and develop the quality of the data transmission.

In the future, the use of integrated optical circuits (PIC) will allow the improvement of the PON networks, since they incorporate different optical components with various functions. The characterization of these chips is still in an early stage in our laboratories and needs to be optimized.

Thus, this work addresses tests that have been carried out to establish a testing model and present a generic test setup. This can be used as a tool with all the necessary stages to the completion of the tests.

It starts with the theoretical framework about PON and the integrated optical circuits. Then, there is a chapter dedicated to measures theory and proper treatment of data obtained in an experiment. Some of the PICs tests performed in the laboratory are presented. Finally, a generic test setup and a test model are suggested. As shown in this essay, the recommended setup is less time consuming, and it offers a higher quality in the data receiving and processing.

This work was supported by FCT under the project COMPRESS - PTDC/EEI-TEL/7163/2014 and the European Regional Development Fund (FEDER), through the Regional Operational Program of Centre (CENTRO 2020) of the Portugal 2020 framework [Project HeatIT with Nr. 017942 (CENTRO-01-0247-FEDER-017942)].

Contents

List of Figures

List of Tables

Acronyms

Al	Aluminium
APD	Avalanche Photo Diodes
As	Arsenide
ATM	Asynchronous Transfer Mode
ATM-PON	Asynchronous Transfer Mode-based Passive Optical Network
AWG	Array Waveguide Grating
BPON	Broadband Passive Optical Network
DBR	Distributed Bragg Reflector
EPON	Ethernet Passive Optical Network
FPR	Free Propagation Region
FSAN	Full-Service Access Network
FSR	Free Spectral Range
FTTB	Fiber to the Building
FTTH	Fiber To The Home
FTTx	Fiber to the X
Ga	Gallium
GPIB	General Purpose Interface Bus
GPON	Gigabit-capable
IC	Integrated Circuit
IEEE	Institute of Electrical and Electronics Engineers
InP	Indium Phosphide
IP	Internet Protocol
NG-PON2	Next-Generation Passive Optical Network 2

OLT	Optical Line Terminal
ONU	Optical Network Unit
OSA	Optical Spectrum Analyzer
P	Phosphorus
P2MP	Point-to-Multipoint
PC	Personal Computer
PCB	Printed Circuit Board
Phasar	Phased Arrays
PIC	Photonic Integrated Circuits
PIN	$p-i-n$ Photodiode
PON	Passive Optical Network
POS	Passive Optical Splitter
Si	Silicon
SOA	Semiconductor Optical Amplifiers
TDM	Time Division Multiplex
TEC	Temperature Controller
TWDM-PON	Time and Wavelength Division Multiplexed Passive Optical Network
WDM	Wavelength Division Multiplex
WGR	Waveguide Grating Router
XG-PON	10 Gigabit Passive Optical Network

Chapter 1

Introduction

1.1 Overview and Motivation

In our days, the demand for higher bandwidth is increasing rapidly due to the emergence of multimedia applications such as video-on-demand or internet services. Therefore, it is necessary to upgrade and find new technologies to accommodate the bandwidth request of new applications. This leads to optical fiber networks [1]. Fiber-optic communication systems are light-wave systems that employ optical fibers with the purpose of exchanging information. Such systems have been deployed worldwide since 1980 and have been revolutionizing the technology behind telecommunications [2].

All of this evolution motivate the introduction of the Fiber-to-the-Home (FTTH) concept to provide new high-speed services. Passive optical network (PON) is one of the various FTTH implementations that have become a good solution for access networks because of the point-to-multipoint (P2MP) architecture and the low-cost components. Conventional PONs are evolving to carry two-way broadband interactive data signals. Bandwidth demands in both enterprise and residential broadband access networks have been increasing drastically and the services carried on PONs are becoming essential to today's deep fiber access solutions [2]. The Next Generation of Passive Optical Networks (NG-PON2) is the last evolution of PON and it is capable to provide 40 Gb/s and keeping compatibility with previous PON versions [1].

The expected FTTH deployment requires low-cost equipment for the customer terminals, where the integrated optics play an important role [3]. Integrated technology for optical devices has been developed within optical fiber communications so that it is now possible to fabricate a complete system onto a single chip. A Photonic Integrated Circuit (PIC) is the monolithic integration of several functionalities on the same optoelectronic chip. The multiple optical elements are fabricated at once on the same chip with many chips per wafer. The PICs can perform not only optical signal guiding and coupling but also controlling functions such as switching, splitting, multiplexing and desmultiplexing of optical signals [4].

Highly sophisticated application-specific methods are developed and used to analyze these chips [5]. In our laboratory, however, with the available material, the measurements can be imprecise and may suffer from systematic errors. The aim of this work is to propose an alternative measurement method and create a test protocol for any PIC tester.

1.2 Objectives

The main objective of this work is to propose a generic test setup and a test protocol for PIC testing. To accomplish that the next objectives were explored:

- Present an overview of passive optical networks and PICs;
- Study of measurement analysis;
- Study the difficulties associated to PIC testing;
- Work with an auto-alignment controller;
- Propose a generic test setup with a valid test protocol.

1.3 Structure

This thesis is divided in six main chapters including this introductory one. The document is organized as follows:

- **Chapter 2 - Passive Optical Networks and Photonic Integrated Circuits** contains some information about PONs, their basic concept, and their evolution. In the second part, the notion of integrated optics is introduced and the main optical components are described.
- **Chapter 3 - Measurement Concepts in PICs** gives the reader an overview on measurement concept and error sources during measurement.
- **Chapter 4 - Experimental Tests** presents the tests done to reach a generic test setup. It is separated in electrical domain PIC test, optical domain PIC test, optical fiber auto-alignment test and total automatization PIC test.
- **Chapter 5 - Generic Testing Methodology** presents the proposed generic test setup and the test protocol based on the experiments performed.
- **Chapter 6 - Conclusion and Future Work** provides a summary of the work done and the main conclusions; in the end, future work to be developed in PIC testing is proposed.

1.4 Contributions

The main contributions of this work are:

- Optical auto-alignment using the controller MMR602 ATP Modular Rack;
- Development of a generic test setup for PIC;
- Propose a protocol for PIC testing.

Chapter 2

Passive Optical Networks and Photonics Integrated Circuits

Chapter 2 is divided in three parts. The main objective of this chapter is to present an overview on PON evolution and PICs. Section 2.1 presents the basic concepts about PON, the multiple access techniques for upstream and finally the main types of PON networks are described.

In Section 2.2, a brief introduction to PICs will be given, also their fabrication and the presentation of some PICs that are available in the market. Section 2.3 presents the optical components that compose the PIC in study, a brief introduction to each one and the main characteristics of them.

2.1 Passive Optical Networks

PON are passive optical networks that connect the supplier to the customer location with a Fiber-to-the-X (FTTx) architecture. Where FTTH refers to users (Fiber to the Home) and FTTB refers to larger companies or buildings (Fiber to the Building). These networks are only composed by passive components, so they do not require electrical energy, presenting advantages in terms of power and heat. The main components used in this networks are the Optical Line Terminal (OLT) located at the supplier, the Passive Optical Splitter (POS), placed between the supplier and the customer, and the Optical Network Unit (ONU) placed in the destination. [6]. There are two crucial points in scaling PON networks: The location and configuration of the OLT and the location of the POS. The POS allows to distribute the optical signal to the several end users.

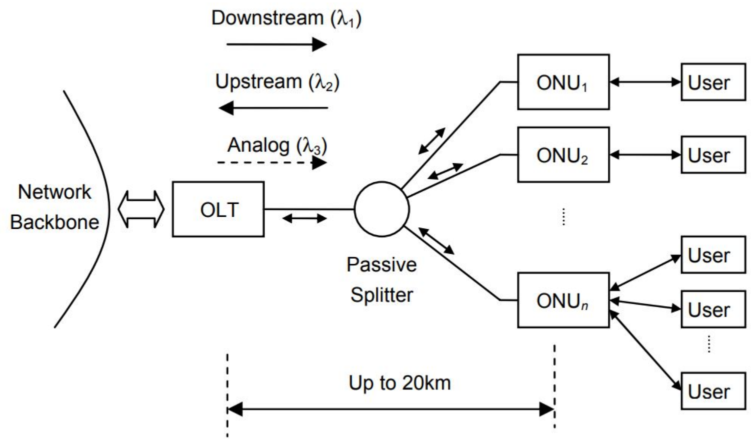

Figure 2.1: Typical passive optical network architecture [7].

There are three ways to implement a PON network:

Bus Topology

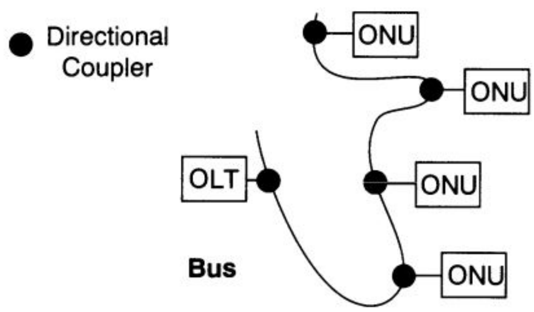

Figure 2.2: Example of a bus topology in PON [8].

This system has a point-to-point connectivity between the OLT and the ONU and each ONU is connected to the fiber via a directional coupler. The main disadvantage of this topology is that one failure in the main fiber is enough to cause disconnection of all users. The bus topology is mainly used for FTTH and especially in rural areas where the distance between users is higher.

Ring Topology

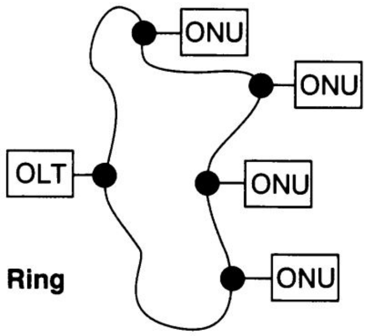

Figure 2.3: Example of a ring topology in PON [8].

This topology is similar to the previous one, but in this case the end and the beginning are connected. The main advantage of this topology is the higher security. If there is a failure in the fiber the traffic circulates in the opposite direction. The main disadvantage is that a passive ring is not easy to produce, because the signal must be removed selectively from the ring after one circulation, being impossible with passive components [8].

Tree Topology

An example of this topology was already shown in Figure 2.1. This is the most used topology. The other two topologies have a mutual disadvantage that is the optical power splitting ratio. Either couplers with the same ratio are used for all stations, which leads to very low received power at the farthest stations, or couplers with tuned ratio are used to give the same power to each of the stations [8]. Another advantage of the tree topology is the cost, it uses less components than the others topologies.

2.1.1 Multiple Access Techniques

With the progress of the networks, the emerging optical access network must provide the bandwidth demand for each user as well as the support high data rate, broadband multiple services and flexible communications for various end-users [9]. It is necessary to control the channel multiple access in the upstream transmission in the PON networks. Time Division Multiplex (TDM) and Wavelength Division Multiplex (WDM) techniques are employed in PONs for higher resource efficiency and capacity.

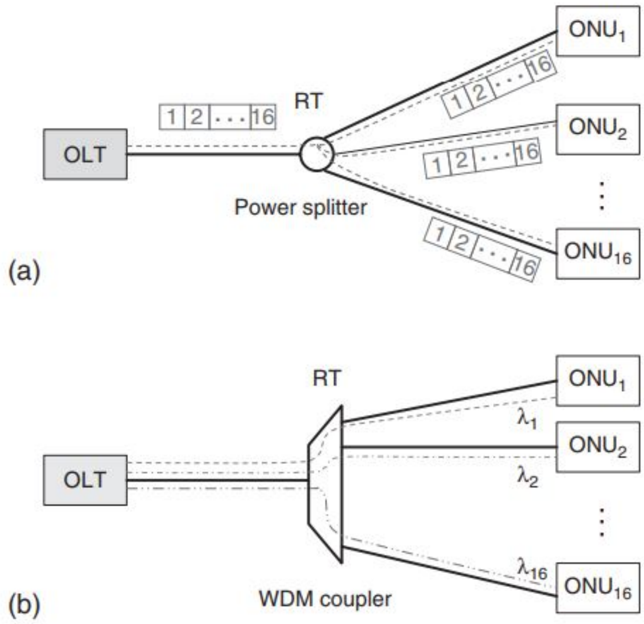

Figure 2.4: TDM-PON in a) and WDM-PON in b) [10].

Figure 2.4 shows the two types of multiplexing architectures. WDM-PON uses a different wavelength for each ONU. Each ONU can simultaneously transmit packages in the same direction using all the available bandwidth, with no need or obligation to share. When a new ONU is introduced it should operate at a different wavelength from others that have already been registered. The advantages of this technique are the very high bandwidth, the simplicity of its implementation and the privacy due to the own wavelength of each ONU. The disadvantage is the high cost and consequently very restricted.

TDM-PON divides the total bandwidth for several channels. The distribution of bandwidth through the channels is done by dividing the time and assigning each to one of them. The OLT is responsible for controlling the ONUs transmission to ensure that there is no collision between the packages. The great advantage of this technique is the lower cost because of the use of a single wavelength throughout the operation. The disadvantage is that this technique is more difficult to manage than the other. Most of the commercial PONs (including BPON, GPON, EPON, and NG-PON2) fall into this type of multiplexing division [10].

It is possible to combine the above two techniques for a better performance in accessing networks. This technique is favorable because it is possible to add new users without the need to include new hardware.

2.1.2 PON Networks Evolution

Several alternative architectures for TDM-PON-based access networks have been standardized by several standard bodies in the past years [11]. The first PON system that achieved commercial deployment was the Asynchronous Transfer Mode-based Passive Optical Network (ATM-PON). In 1995, the Full-Service Access Network (FSAN) was formed with the objective of creating a unified specification for broadband access networks, so ATM-PON was created based upon access network that uses an Asynchronous Transfer Mode (ATM) as layer-2 protocol. With the traffic evolution, ATM-PON couldn't support services like Ethernet access, video distribution or virtual private line so it needed to evolve that's why Broadband PON (BPON) was created. The original BPON system has a 155 Mbps upstream and downstream bit rates [11], but these values were improved to 155 Mbps upstream and 622 Mbps downstream.

With the explosion of internet and intranet-based traffic in the years following, ATM-based BPON systems proved to be very inefficient, as the vast majority of traffic through the access network consisting of variable length IP traffic [12]. As a result of the creation of a pure Ethernet-based PON (EPON). EPON is based upon IEEE 802.3 Ethernet that was modified to support Point-to-Multipoint (P2MP) connectivity [12]. This system distributed downstream at a rate of 1Gb/s with a wavelength of 1490 nm and upstream at a rate of 1 Gb/s with a wavelength of 1310 nm, being the wavelength of 1550 nm reserved for analog video transmission. In this networks, in order to connect a new ONU, the OLT periodically opens a window of time specifically with this purpose and waits for the manifestation of the ONU.

In the ever-growing traffic volume and the emergence of 1 Gbps EPON specification, the FSAN group realized the need for a kind of architecture capable of higher bit rate and improved efficiency for data traffic. [11]. The development of the Gigabit-capable Passive Optical Network (GPON) gave a dual Gigabit speed ATM/EPON solution that distributes downstream at a rate of 2.488 Gbit/s with a wavelength of 1490 nm and a budget link of 28 dB. In upstream uses a rate of 1.244 Gbit/s with a wavelength of 1310 nm and a link budget of 28 dB. The OLT is responsible for determining the distance and the delay for each user. The splitters in this type of network can be 1:32, 1:64 or 1:128.

In 2010 with the growing demand for network, was developed the 10 Gigabit Passive Optical Network (XG-PON) the last version of the GPON. This version can support 10Gbps for downstream and 2.5Gbps upstream. This evolution can also support a higher split ratio of 128 users per PON and a power budget range of 29 dB to 31 dB, being possible to reach 33 and 35 dB in extend class [13].

The latest version of PON networks is the Next-Generation Passive Optical Network 2 (NG-PON2) developed in 2015 to overcome the bandwith demand and the costs of the XG-PON. Provide an architecture capable of 40 Gb/s downstream capacity, divided by four 10 Gb/s signals multiplexed with a 10 Gb/s upstream capacity. Recently, studies have been carried out on NG-PON2 enabling technologies, such as , wavelength division multiplexed PON (WDM-PON) or time and wavelength division multiplexed PON (TWDM-PON). TWDM-PON has been selected as the best candidate for NG-PON2 because it supports backward compatibility, flexibility, static sharing and the large split ratio offered which helps in achieving lower cost and power consumption per user [1].

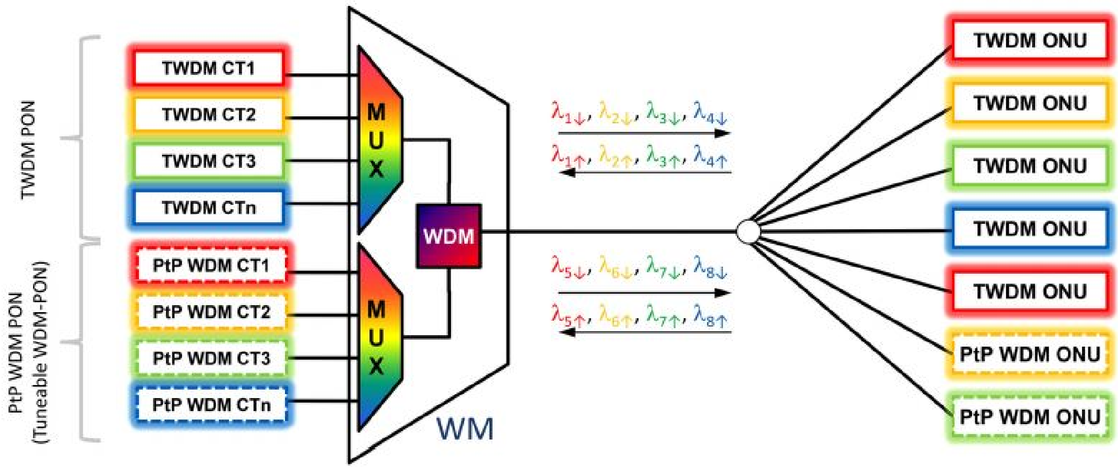

Figure 2.5: NG-PON2 system architecture [14].

NG-PON2 can support a reach of a least of 40 km and will reach 60-100 km with reach extenders in the future. NG-PON2 must be able to operate over the same passive infrastructure previously defined for GPON and XG-PON. The wavelength used is 1524 nm to 1544 nm in upstream and 1596 nm to 1602 nm in downstream [14].

2.2 Photonic Integrated Circuits

The idea of integrated optics circuits (now usually named Photonic integrated circuits (PICs)) appeared for the first time in the early 1970s, inspired by the success of the electronic integrated circuits (ICs). It could drastically reduce packaging cost, enhance power budget by suppressing lossy optical couplings and lower critical power among several functionalities [3]. PIC eliminates the needs of a large number of optical components and complex electronic signal processing, achieving great network reliability [15].

In PIC fabrication first, a common substrate is chosen. The substrate is selected between indium phosphide (InP), Silicon (Si) or TriPleX (combination of Silicon Nitride – Si3N4 and Silicon Dioxide – SiO2), and thin layers of a semiconductor crystal materials are deposited. The InP substrate it is the most used because can be monolithically integrated with active devices. The InP substrate gives efficient optical gain, high-speed switching, modulation with low voltage and efficient high-speed detection [15]. The thin layers are also composed of elements from columns III and V of Mendeleev's table: Gallium (Ga), Arsenide (As), Phosphorus (P) or Aluminium (Al) [3]. In optical communication, the PIC can integrate many types of functionalities as mainly optical passive waveguiding, optical amplification (gain), signal generation (amplitude or phase modulation), or photodetection. Each functionality is achieved with a specific material choice and electrical operation mode [3].

The PICs development differs from small-scale PICs to large-scale PICs. The small-scale PICs can integrate laser-modulator or tunable lasers, the large-scale PICs can implement new modulation formats Tx/Rx, multi-channel Tx/Rx, or even complete sub-systems [3].

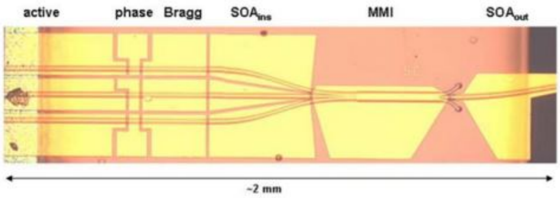

Figure 2.6: Example of a Small-Scale PIC [3].

Figure 2.6 represents a small-scale PIC constituted by a DBR laser with an SOA amplifier. The first company to accomplish the fabrication of a large-scale PIC was Infinera's. The proposed PIC in the transmitter (Tx) has 10 channels of 10 Gb/s optical signals, each converted from electronic inputs and multiplexed into a single output fiber. The receiver (Rx) has 10 outputs channels with 10 Gb/s electronic signals, each channel is converted from an optical signal by a demultiplexer and an array of waveguide photodetectors[16]. The block diagram of the 10 × 10 Gb/s Tx/Rx Infinera's chip is represented below in Figure 2.7.

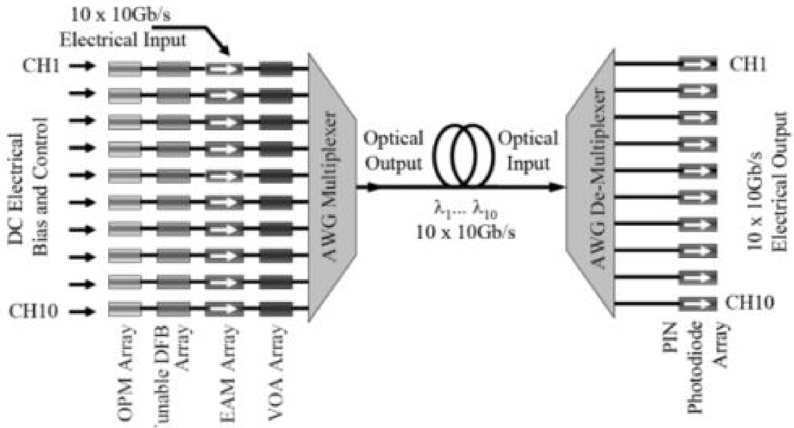

Figure 2.7: Block diagram of 10 × 10 Gb/s Tx/Rx Infinera's chip [3].

Although the levels of complexity and sophistication in PIC have increased over the years, most of the large-scale PICs have not been commercialized successfully. The only reported success was the 10 × 10 Gb/s Tx/Rx Infinera's PIC [17]. In the future it is expected to see more PIC being developed, constituted by more components but with the decrease in size, making it possible to process more signals and have lower losses.

2.3 Optical Components

Photonic integrated circuits refer to the fabrication and integration of several components into a single planar substrate. The main components in a PIC are splitters, couplers, gratings, polarization controllers, interferometers, sources, detectors or optical amplifiers.

The optical components are divided into two groups. The active components that require some type of external energy to operate on signals and the passive components that don't need any input power to work. In this section it will only be presented the Array Waveguide Grating (AWG) and the Photodetector, because these are the main components analysed in the scope of this dissertation.

2.3.1 Array Waveguide Grating

The Array Waveguide Grating, also known as AWG, is a multiplexer or desmultiplexer based on an array of waveguides. First reported by Smit in 1988, it has different designations: Phased Arrays (Phasars), Arrayed Waveguide Gratings (AWGs), and Waveguide Grating Routers (WGRs) [18]. AWG is the most important filter type in photonic integrated circuits.

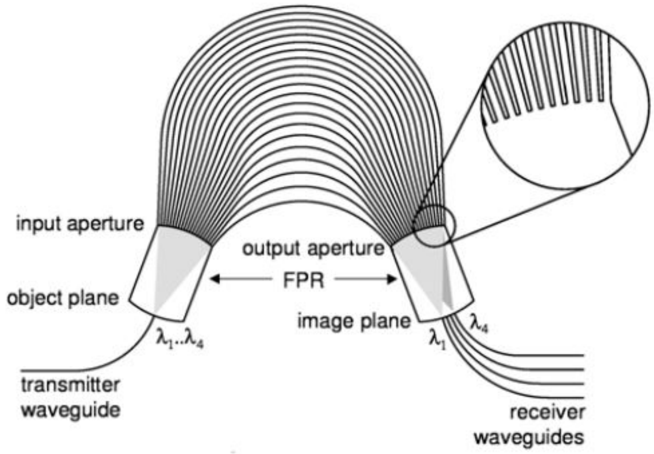

Figure 2.8: Example of a AWG demultiplexer 1x4 [18].

Consists in one input waveguide, several output waveguides and two focusing star couplers slab waveguides (also called free propagation region) which are connected via an arrayed-waveguides with a constant path length difference between them [19]. When a beam propagating through the transmitter waveguide enters the Free Propagation Region (FPR) area is no longer laterally confined and becomes divergent. On arriving in the input aperture the beam is coupled into the waveguide array and propagates through the individual waveguides towards the output [18]. In the beginning, it was only possible to implement an AWG with 1 input and N outputs, nowadays with the development of the integrated optical study it is possible to have N inputs and N outputs.

In AWG the length difference ΔL between adjacent waveguides is equal to an integer number m of wavelengths inside the AWG:

$$\Delta L = m\frac{\lambda_c}{n_{eff}} \tag{2.1}$$

Where m is the the order of the array, n_{eff} is the effective refractive index of the waveguides, and λ_c is the central wavelength. The length increment δL of the array gives rise to a phase difference according to [18]:

$$\Delta\phi = \beta\Delta L \tag{2.2}$$

The variable β is the propagation constant in the waveguides and it is given by:

$$\beta = \frac{2\pi\nu n_{eff}}{c} \tag{2.3}$$

Where ν is the frequency of the propagation wave, and c is the light speed in vacuum. If the change in the input wavelength is such that the phase difference $\Delta\phi$ between adjacent waveguides has increased by π, the transfer will be the same as before and the response of the AWG is periodic [18]. In the frequency domain the period between two successive fields is called Free Spectral Range (FSR) represented by the following relationship [19]:

$$FSR = \frac{\nu_c}{m}\left(\frac{n_{eff}}{n_g}\right) \tag{2.4}$$

in which n_g is the group index mode of the waveguide. The parameter FSR is shown in Figure 2.9.

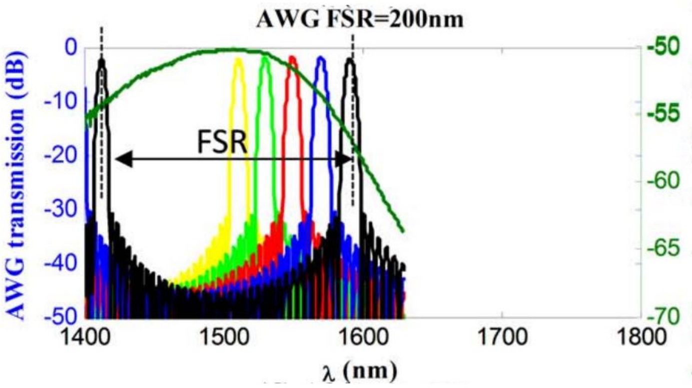

Figure 2.9: Example of the FSR parameter [5].

In characteristics, an AWG mux/demux device has lower loss, flatter pass-band and it is easier to realize on an integrated optic substrate [19].

When is required an analysis of the component one of the most important characteristics is the temperature dependence. The main effect of a temperature change in an AWG is the shift of the wavelength response, the InP-based AWG has a dependence on the order of the 0.12nm/ºC [18].

Fields propagating through an AWG due to various losses are attenuated. Those losses have their origin in the junctions between the free propagation regions and the waveguide array. We have three major parameters to measure the error introduced in the AWG. The crosstalk, that is defined as the difference between the maximum transmission of an AWG channel and the crosstalk floor. In an InP-based AWG, the typical crosstalk is in the order of -25dB. The roll-off, that is defined as the insertion loss of the outer channel with respect to the central one and the central wavelength shift that it is the difference between the desire and the measured AWG central wavelength [5].

2.3.2 Photodetectors

In an optical connection, the component responsible for the conversion of the electrical signal into an optical signal is the optical transmitter. The signal after coupled in the fiber travels long distances needing at the destination a conversion of the optical domain for the electrical domain. This conversion to photons into electrons is done by an optical receiver (photodetector). In order to have a good efficiency in the receiver, it is needed that the photodetector has a sensitivity at the required wavelength, low noise, sufficient area for efficient coupling to optical fiber, low cost and high reliability. In fiber optics, two types of photo detectors are of primary interest: PIN diodes and Avalanche Photo Diodes (APD) [7].

The principle of operation behind photo detectors is the light absorption. An incident photon creates a free pair, removing an electron from its atom (ionization). The probability of absorption depends on the depletion width, the material coefficient, the incident light, the number of photons lost to the depletion region and the surface reflection. To occur absorption the energy hv of the incident photons needs to exceed the band gap energy, E_g. Figure 2.10 represents the absorption effect in a photodetector.

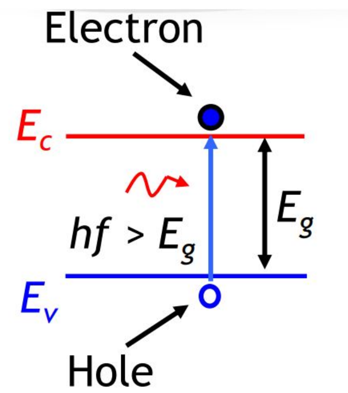

Figure 2.10: Schematic of the absorption effect [20].

Under the influence of an electric field set up by an applied voltage, electrons and holes are swept across the semiconductor, resulting in a flow of electric current (I_p) that is proportional to the incident optical power (P_{i_n}) [2].

$$I_p = R \times P_{i_n} \tag{2.5}$$

Where the constant R is the responsivity and can be expressed in terms of the quantum efficiency (η). The quantum efficiency is the probability that an incident photon will produce an electron-hole pair and is given by:

$$\eta = \frac{hv}{q} R \tag{2.6}$$

Where q is the electron charge and h the Planck's constant. The responsivity gives the transfer characteristic of the detector and it is the ratio between the output current and the input optical power, depending on the wavelength of the incident light, the applied bias voltage, and temperature [4].

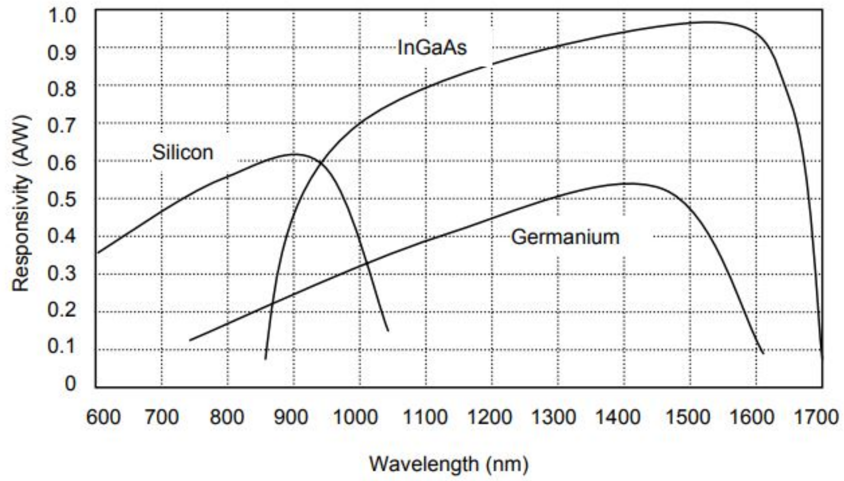

Figure 2.11: Dependence of responsivity with the wavelength and material [7].

From Figure 2.11 is seen that the responsivity varies with the wavelength. At longer wavelengths, responsivity drops abruptly because the photons do not have enough energy to knock electrons from the valence band to the conduction band. At lower wavelengths the responsivity also reduces because of increased absorption [7].

The probability that an incident photon will produce an electron-hole pair can also be written as:

$$\eta = \frac{P_{abs}}{P_{in}} = 1 - exp(-\alpha\, W) \tag{2.7}$$

Where P_{abs} is the absorbed power and α is the absorption coefficient. The absorption coefficient is strongly dependent on wavelength, as shown in Figure 2.12.

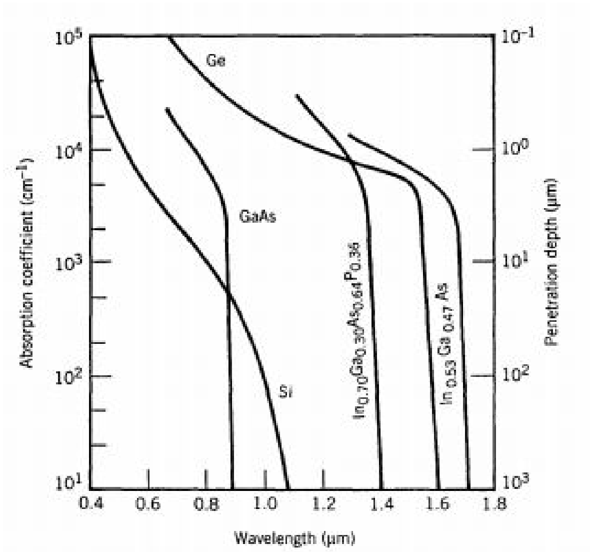

Figure 2.12: Wavelength dependence of the absorption coefficient for several materials [2].

As seen, when α is zero the cut-off wavelength (λ_c) is reached and the material can be used as photodector only for $\lambda < \lambda_c$ [2]. There are many types of photodetectors, but the ones considered in this thesis will be the PIN and the APD.

The PIN photodiode consists of an intrinsic region sandwiched between p and n-type layers, as shown in Figure 2.13. Typically, reverse biased like a photodetector. Because of its intrinsic nature, the middle layer offers a high resistance, and most of the voltage drop occurs across it. As a result, a large electric field exists in the i-layer [2]. This region causes a significant increase in the absorption of incident light and an increase in the quantum efficiency of the photodetector.

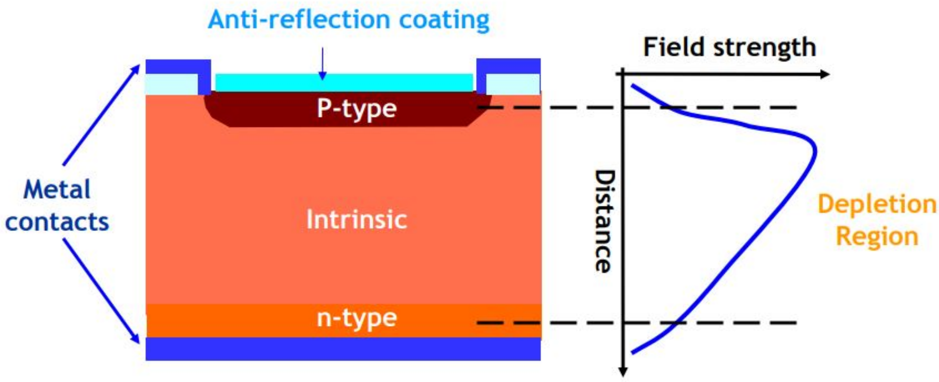

Figure 2.13: Structure of a PIN diode [20].

When photons hit the intrinsic region, they cause valence band electrons to jump into the conduction band leaving a positive charge (hole) behind. Thus, a population of photo-generated carriers is created in the intrinsic region. These carriers drift out of the intrinsic region because of the present electric field. This drift causes the holes to move toward the p-region and the electrons move toward the n-region with opposite direction. Which leads to an electric current flow [7]. The speed of movement performed by the holes and electrons is limited by the diffusion time of carriers outside the depletion region, the time constant of the p-n junction capacitance and the photodetector load resistance [20].

The APD is a improved structure PIN photodiode that creates an extremely high electric field region called the avalanche region. This region accelerates the carriers causing a high collision energy releasing the connected electrons. These free electrons can collide and release more energy. This process is known as avalanche multiplication resulting in a high gain current. In Figure 2.14 is shown a popular APD structure.

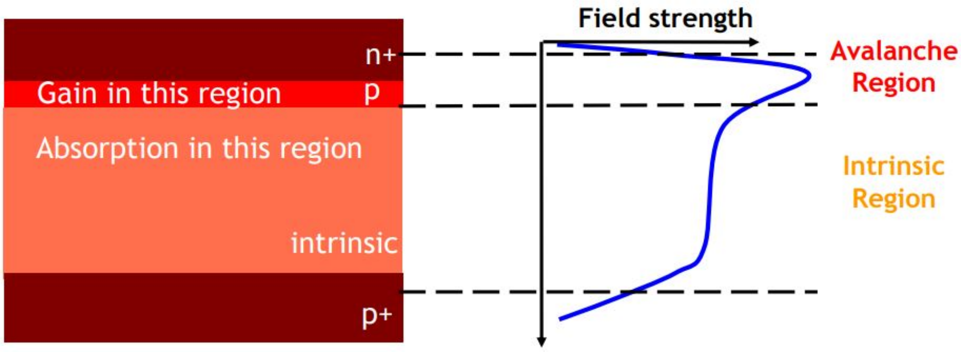

Figure 2.14: Structure of a APD diode [20].

The APD structure consists in a highly doped p+ and n+ regions on either side of a lightly doped. There is also an additional *p* layer sandwiched between the n+ and p regions.

The advantages of the APD relatively to the PIN is that the first one has gain, so it can detect weaker signals. In the disadvantages the APD requires a higher bias voltage than a PIN, is noisier, more expensive and is more sensitive to variations in temperature and bias voltage [20].

Chapter 3

Measurement Concept

Being the goal of this thesis the study and the propose of alternative measurement methods in photonic integrated circuits, an understanding of measurement theory is required. Chapter 3 presents a study regarding measures and their associated errors. In the first section, it will be described the meaning of measure and the difference between direct and indirect measures. In the second part of this chapter it will be addressed the concept of error associated with the measurements made and the propagation throughout the experiences.

3.1 Measurement Theory

Measurement is the process, that, after an objective observation assigns a numerical value to a natural entity [21]. The measurement instrument will compare the variable that is being observed with another that serves as a reference. In an ideal measurement, the value is assigned to every single observation of a phenomenon. Real measurement procedures, on the contrary, are affected by errors what reduce the final measurement accuracy [5].

The final result of a measurement can be demonstrated in two ways:

$$\text{Measurement} = \text{numerical value} \pm \text{absolute error (units)} \tag{3.1}$$

$$\text{Measurement} = \text{numerical value (units)} \pm \text{relative error (\%)} \tag{3.2}$$

The measurements performed can be dynamic or static. Static measurement when through the measurement the value is not variable. Dynamic measurement when calculating the instantaneous value of a magnitude or its variation over time. The measuring methods can be divided in direct and indirect methods.

The direct measurement method is any measurement where the numerical value assigned to the entity of interest is directly measured (read) at the instrument. In a photonic integrated circuit, an example is the optical power curve measurement [5]. The indirect measurement method is any measurement obtained through other numerical values (direct measures) via a numerical relation between them. An simple example that will be used in this thesis is the Ohm Law:

$$R = \frac{V}{I} \tag{3.3}$$

In this example, the resistance (R) is obtained by a numerical relation between two direct measures. The voltage (V), measured in a voltmeter, and the current (I), measured in an ammeter.

After collecting the experimental results it is necessary to make an assessment of them, to know if they are reliable and correspond with the expected. This evaluation has two methods: the first is the precision that corresponds to realize the experiment without knowing the real value of the parameter but rather an approximation. A result is more precise, then lower is the relative error [22].

$$\text{Relative Error} = |\frac{\Delta x}{x}| \times 100\,(\%) \tag{3.4}$$

The other method is the accuracy that is the degree of agreement between the measurement result and the value (conventionally) true of entity measured [21]. In the most documentation, a measure is more precise when the relative error is less than 10%.

Also in the evaluation of results, when it is obtained a high number of samples, sometimes it is necessary a study on the variation of them (dispersion). For this graphical methods are used, like the histograms [23]. For the construction of a histogram three steps are needed:

1. The group of measures is divided into intervals of a given amplitude (also called class). A typical value for this interval is the error associated with each of the individual measures;

2. Counts the number of results x_i that occur in a given interval (occurrence frequency, $f(x_i)$)

3. The graph $f(x)$ is plotted as a function of the intervals.

When the measurements number is small ($N < 10$), there is no need for studying the dispersion of the sample around the mean and estimating the standard deviation. The best method is to consider the uncertainty in the measurement as the maximum of the deviations $d_i = |x_i - \overline{x}|$. And then the final value will be [22]:

$$X = \overline{x} \pm \{Max\, d_i\} \tag{3.5}$$

Where the $\overline{x}$ is the mean value and represents the most probable value.

$$\overline{x} = \frac{x_1 + x_2 + ... + x_N}{N} \tag{3.6}$$

3.2 Error Source

As previously seen, any measurement performed is affected by errors. These errors can be distinguished by two sources. The first errors are related to the measurement procedures and/or the assemblies made that correspond to the direct measurements. The errors introduced by the mathematical relationships between the parameters correspond to the indirect measures [24].

3.2.1 Direct Measurement Method

During direct measurements the values are read directly on the measurement instrument, so the error corresponds to the one read in the device:

- In the analog instruments is the half of the smallest reading range;
- In the digital instruments is the lower scaling.

In direct measures there is another error source, that is when the interaction of the observer with the instrument is not correct. Example of this error may be the time response when the measurement is performed or the incorrect positioning in relation to the scale of the instrument. Another factor that can influence the direct measurements is the deficient calibration of the instrument not guaranteeing, the correct scales according to the standards used.

Thus, errors related to direct measures can be divided in two groups. Systematic errors, where are constant and affect all measurements made, for example, a calibration error, and random errors where the same measurement is made and are obtained different results, in this case, an example may be a deficient observation [21]. In laboratory experiments, these two types of errors can happen simultaneously.

3.2.2 Indirect Measurement Method

Indirect measurements are a two-step process. First, the secondary parameters are measured, followed by the relation between the secondary and the primary parameters through mathematical expressions. The errors made in the measures propagate in the second phase. Suppose that to determine the variable F measurements were taken independent of the quantities x, y, z, such that:

$$F = f(x, y, z) \tag{3.7}$$

Considering that each one parameter have an associated error δ_x, δ_y e δ_z, the value of the error in the measure is calculated using the concept of the derived from a function.

$$\delta F = \left(\frac{\partial F}{\partial x}\right)_{(\overline{x},\overline{y},\overline{z})} \delta x + \left(\frac{\partial F}{\partial y}\right)_{(\overline{x},\overline{y},\overline{z})} \delta y \left(\frac{\partial F}{\partial z}\right)_{(\overline{x},\overline{y},\overline{z})} \delta z \tag{3.8}$$

Where $\left(\frac{\partial F}{\partial x}\right)_{(\overline{x},\overline{y},\overline{z})}$, $\left(\frac{\partial F}{\partial x}\right)_{(\overline{x},\overline{y},\overline{z})}$ e $\left(\frac{\partial F}{\partial x}\right)_{(\overline{x},\overline{y},\overline{z})}$ are respectively the derived parcials of the function F in relation to the variables x, y and z. This represents the total diferencial of the function F calculated in the point $(\overline{x}, \overline{y}, \overline{z})$.

When the number of the measures to determine x, y, z is small we will consider not the partial derivatives but the module of these derivatives [21].

$$\Delta F = \left|\left(\frac{\partial F}{\partial x}\right)_{x,y,z}\right| \Delta x + \left|\left(\frac{\partial F}{\partial y}\right)_{x,y,z}\right| \Delta y + \left|\left(\frac{\partial F}{\partial z}\right)_{x,y,z}\right| \Delta z \tag{3.9}$$

Another situation in the indirect measures that leads to errors is when the experimenter is interested in studying quantities that are not independent of each other and establishing their mathematical expression [24]. The simplest of this relation is the linear (used in the next sections). In this case, the value of the desired quantity is related to the slope and the ordinate at the origin. A linearization is always of the type:

$$y = mx + b \tag{3.10}$$

Where the m is the slope and b the ordinate at the origin. When the quantities do not obey the line equation the equation must be rewritten where the new variables used for the abscissa and ordinate in the new system of axes are linearly related (linearization of a mathematical expression).

In an experiment with few points, the error associated with linearization is given by the expressions below. These expressions involve a statistical parameter r (correlation coefficient) used to evaluate the adjustment to experimental points. In the perfect situation the value should be $r^2 = 1$.

$$\Delta m = |m| \sqrt{\frac{\left(\frac{1}{r^2} - 1\right)}{N-2}} \tag{3.11}$$

$$\Delta b = \Delta m \sqrt{\frac{\sum_n^1 x_i^2}{N}} \tag{3.12}$$

$$r = \frac{N \sum_1^N x_i y_i - \sum_1^N x_i \sum_1^N y_i}{\left[N \sum_1^N x_i^2 - \left(\sum_1^N x_i\right)^2\right]^{1/2} \left[N \sum_1^N y_i^2 - \left(\sum_1^N y_i\right)^2\right]^{1/2}} \tag{3.13}$$

The more efficient and accurate our results are the correlation coefficient (r^2) approaches 1 and to obtain a reliable experience the values of slope and ordinate of origin must be in the intervals $[m - \Delta m; m + \Delta m]$ e $[b - \Delta b; b + \Delta b]$ respectively.

After the study on the measurement concept and its associated sources of errors, it is possible to advance to the testing part and understand the results obtained with the correct analysis.

Chapter 4

Experimental Tests

In photonic integrated circuits, die-level testing is the characterization across the whole chip, which is important in a commercial environment where statistical data and yield are important issues [5]. The final objective of this dissertation is the maximum automation in PIC testing with the resources that are available. The PIC provided for testing consists of an AWG with one input and three output and eight PIN photodiodes, allowing to perform measurements both in the optical and electrical domain in the chip.

This chapter is divided in four parts. In Section 4.1 an optical test will be done with traditional methods, manual optical alignment and data observed in the measurement instruments through the human eye. Using the same PIC an electrical study will be carried out,considering the same conditions as in the previous section (Section 4.2).

In the third Section it will be demonstrated an automatic optical alignment test using the controller Thorlabs MMR602 APT Modular Rack. This controller will be used to correct the errors made by the manual alignment.

In the fourth and last section it will be demonstrated an overall automatic test where the user only needs to organize the data observed in the Personal Computer (PC). The fiber alignment is performed by the controller and the various instruments data will be automatically observed in the PC. All the measures done in this chapter will be analyzed considering the concepts presented in chapter 3.

4.1 Optical Test

The first test will be in the optical domain with manual fiber alignment and data observed in the instrument. The objective of this test is to characterize the AWG, in the optical domain, with one input and three output[1] as indicated in Figure 4.1, and find all the difficulties on measurement. The optical domain test will be divided into two parts, the first will be characterizing and observing the AWG outputs and the second will study the influence of the temperature in the PIC.

[1]The AWG has three outputs but the chip as only two optical outputs.

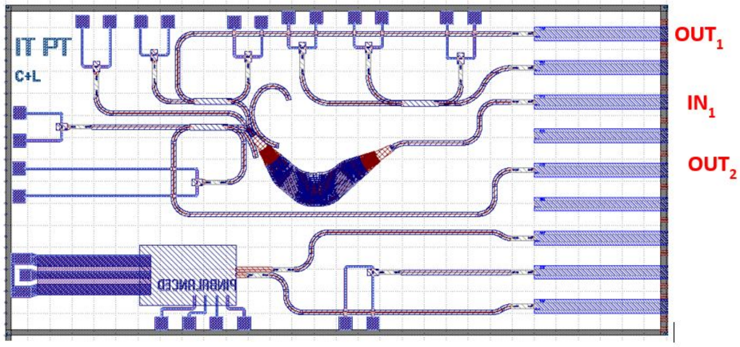

Figure 4.1: Schematic of the PIC under study.

In the input it will be connected an ASE Light Source with a spectrum that covers the C-Band (1530 nm - 1565 nm) and the L-Band (1565 nm - 1625 nm). This ASE has two channels. The first is responsible for the L-Band with a current of 700 mA and the other is responsible for the C-band with a current of 500 mA. Both exits are connected to an Optical Spectrum Analyzer (OSA) being possible to observe the optical power as a function of wavelength. In this experience the PIC is at room temperature of 25°C. The block diagram of the test is shown in Figure 4.2 and a picture of the setup is shown in Figure 4.3.

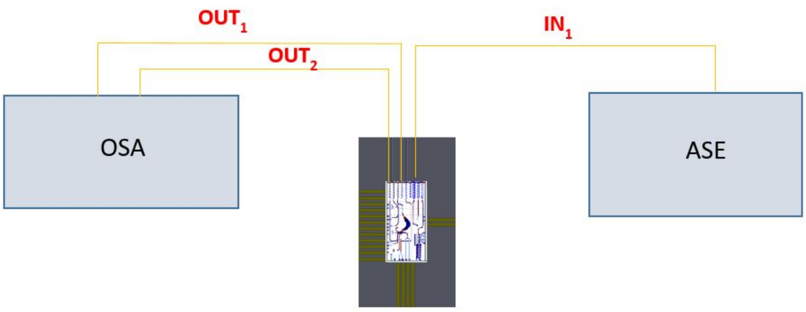

Figure 4.2: Block diagram setup.

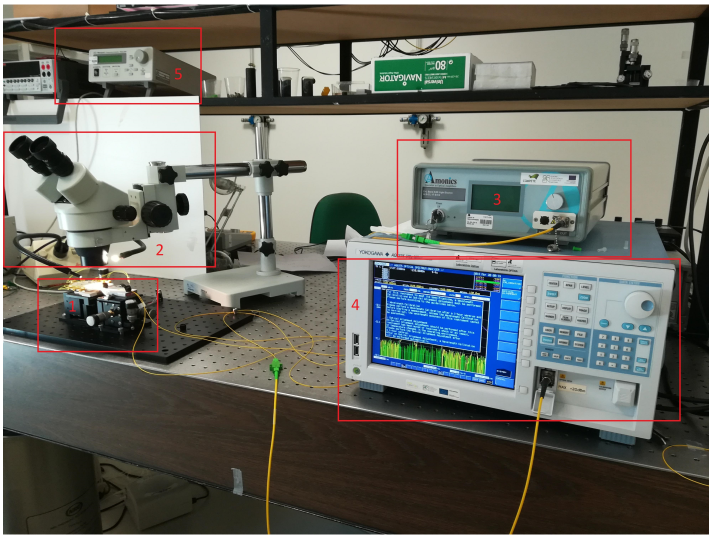

Figure 4.3: Optical test setup.

Number	Category	Model	Brand
1	PIC - Holder - PCB with 3d Stages		
2	Microscope Objective		
3	ASE	ALS-CL-17-B-FA	Amonics
4	OSA	AQ6375	Yokogawa
5	TEC	3040	Newport

Table 4.1: Optical test materials.

The materials needed for this test are shown in Table 4.1 and the numbers have correspondence with Figure 4.3. The number 1 in Table 4.1 is shown with more detail in Figure 4.4 where is possible to see in the left the PIC inside a holder and the holder connected to a PCB. On the right there is a V-groove that ensures that the fiber does not move in the vertical axis. The set PIC-Holder-PCB and the V-groove are each one supported by independent 3D stages.

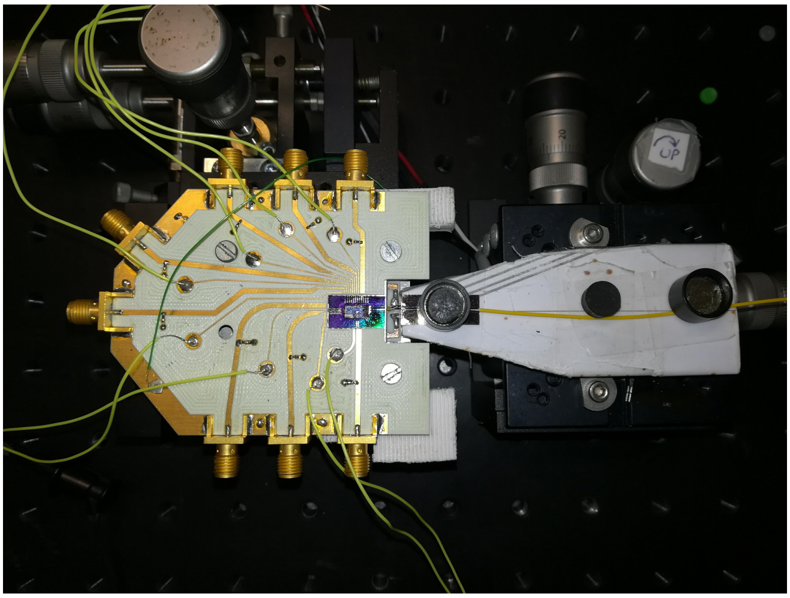

Figure 4.4: PIC in the PCB and the holder.

Figure 4.5 shows the two output signals and the input signal. As mentioned in Section 2.3.1, to measure the accuracy of the AWG we need to consider four major parameters: crosstalk, roll-off, central wavelength shift, and the FSR. As mentioned in the manual of the OSA referred in Table 4.1, all power values have an error value of ± 0.1 dB. The wavelength values have an error of $\pm 0.1\,nm$ which corresponds to the smaller division of the respective digital instrument as seen in the previous chapter.

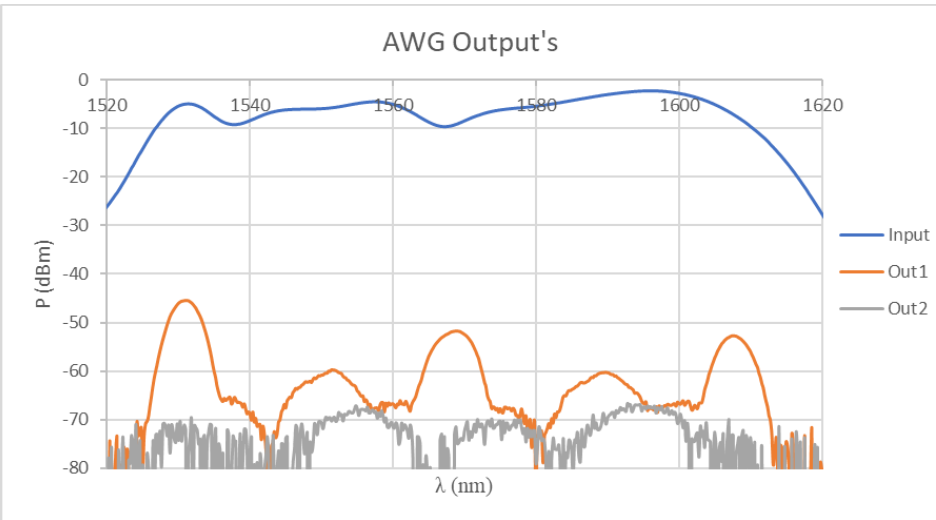

Figure 4.5: Input signal and output signals of the PIC in the optical domain.

This PIC purpose is to perform as an NG-PON2 filter, that divides the upstream (1525 nm - 1545 nm) from the downstream (1595 nm - 1605 nm). It is expected that one output signal of the chip has a maximum in the upstream range and the other output in the downstream range. The output signals are periodic and the interval between the repetitions is the FSR.

Output 1 signal is visible with few distortions in the spectrum, meaning the fiber manual alignment was appropriate, thus it is not the highest error source in this experience. The signal has the first peak around 1535 ± 0.1 nm corresponding to the NG-PON2 upstream, the peaks in 1569 ± 0.1 nm and 1608 ± 0.1nm are repetitions of the first. In theory, all peaks would have the same amplitude and the distance between them would always be the same but as this is a real experience where there are imperfections, this is not possible.

The crosstalk in an InP based chip has a typical value of -25 dB, in this case, has a value of -28.8 ± 0.1 dB with an error percentage of 15.1%. The measured value is considered accurate. The value of roll-off is 6.3 ± 0.1 dB which is a reasonable measurement as the typical value of roll-off in this type of AWG is in the order of 3 dB or higher.

The difference between the two first peaks is 38 ± 0.1 nm and the lasts peaks is 39 ± 0.1 nm, meaning that the third peak has a wavelength shift of 1 ± 0.1 nm. The FSR value chosen to compare with the output 2 is 38.5 ± 0.1 nm [2]. Figure 4.6 illustrates the normalized output 1 signal.

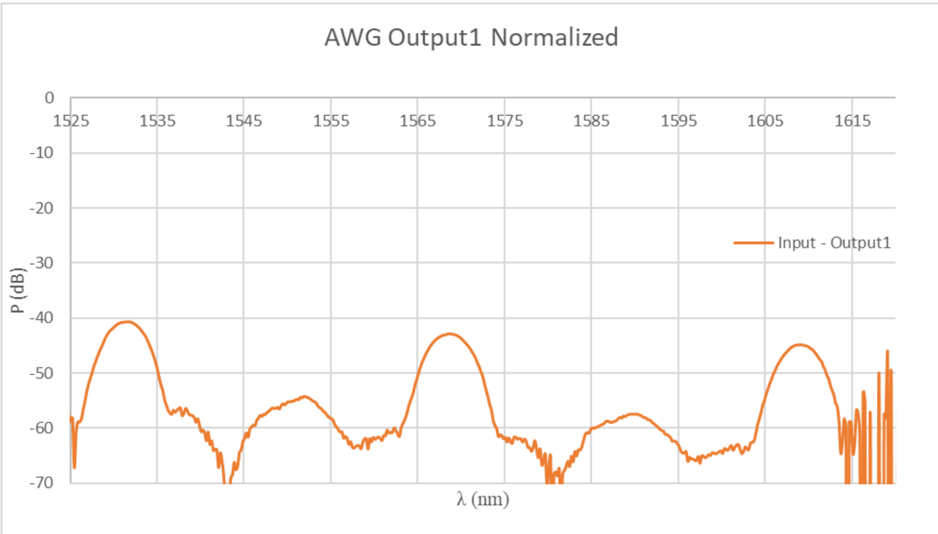

Figure 4.6: Normalized output 1 graphics.

As seen in Figure 4.5 the output 2 signal has a lot of noise along the spectrum, interfering in the OSA optical power measurements. The FSR as seen before is $38,5 \pm 0.1$ nm and the measure one in 39 ± 0.1 nm what is expected, the roll-off is about 1.9 ± 0.1 dB, what is too low but the reason is that the output 2 has a lot of distortions and uncertainties what impairs the measurement.

The crosstalk measure was 26.1 ± 0.1 dB with a percentage error of 4.5% that means is an accurate and exact value.

Figure 4.7 shows the normalized signal of output 2.

[2] Small number of measurements, causing that the FSR final value was calculated using the Equation 3.5.

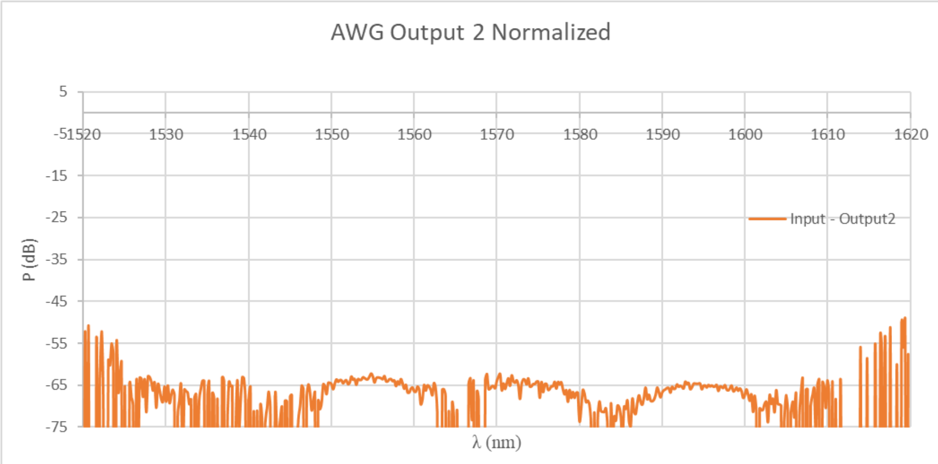

Figure 4.7: Normalized output 2 graphics.

After characterizing both outputs of the AWG, the second part of this test started by studying the influence of temperature on the AWG behavior. To study this behavior a Temperature Controller (TEC) was used. The range considered was between $15°C$ and $55°C$, outside this values the AWG does not have a regular behavior which could interfere with the measurements. The output chosen was the first one because as shown previously it presents the best response.

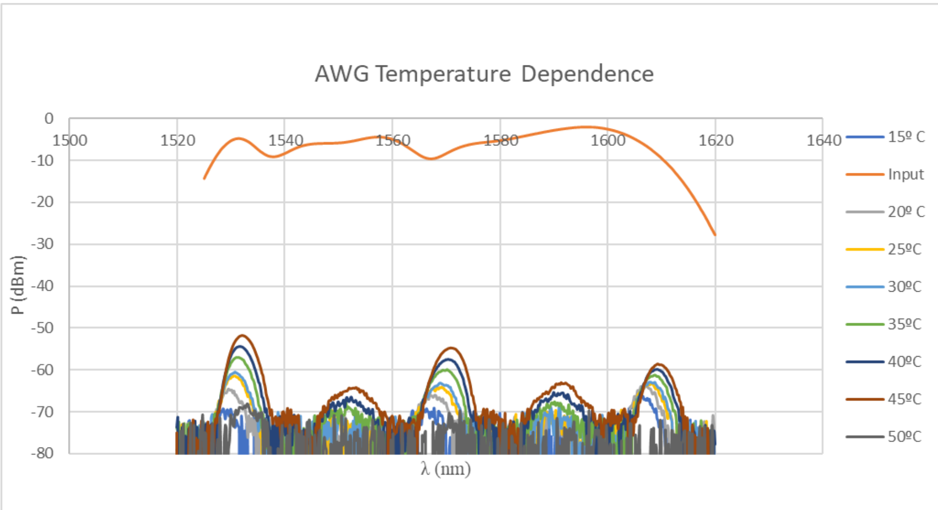

Figure 4.8: AWG output1 temperature dependence.

Figure 4.8 shows the temperature dependence as a function of the wavelength. As observed, while the temperature grows the amplitude of the peaks increases and the central wavelength shifts to higher values, so it is possible to conclude that we have a direct proportionality between the temperature and the maximum transmission wavelength. As explained in Chapter 2 this dependency has a theoretical value of $0.12\, nm/°C$, to search this value was made a linearization between the values of temperature and the first wavelength peak.

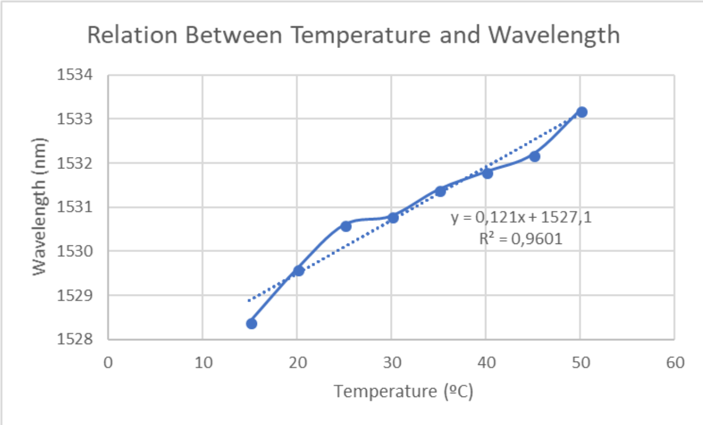

Figure 4.9: Linearization of the relation between the temperature with the first peak wavelength.

Figure 4.9 shows the linearization. The line equation gives a slope value of 0.121 ± 0.01 nm/ºC [3] which is very close to our desired value. Comparing the values we have a percentage error of 0.83% that means that the value is accurate. The error value in the relation between the temperature and the peak amplitude wavelength would be different if we had more points of temperature but was impossible because the output signal for temperatures below $15°C$ and above 50ºC was saturated and very unstable, with noise.

At the end of the experience is possible to conclude that the most challenging difficulties detected in a PIC optical test are the fiber alignment and the measurement reading. Considering manual operation, the probability of error is high. In addition to existing losses in the AWG we always have the human error in both the measures as in the alignment. The OSA used in the experiment has USB interface exits that facilitates the measuring procedure, but the time consuming to get the data in a USB storage media is too long. The output 2 is not stable because of not proper fiber alignment and the waveguide of output 2 has a failure that also causes degradation. For all reasons, the experience gets very delayed that, in big platforms, or in big companies, corresponds to a significant increase in the costs.

4.2 Electrical Test

In the second part of the section, a test will be performed in the electrical domain considering the same PIC. This test consists of the review of the optical power distribution in three photodiodes, each one connected to an exit of the AWG. In the end, the peaks of the signals must agree with the spectra presented in the first section of this chapter.

[3]The calculation of the slope error was using (3.11).

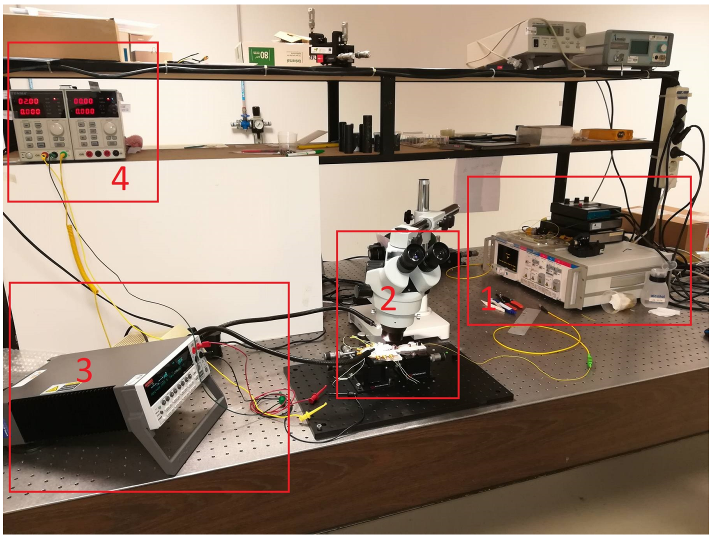

Figure 4.10: Test Setup for the electrical domain.

The setup used for this test is presented in Figure 4.10. Number 1 presents the lasers that were used for the wavelength scanning. The first laser used was the Yenista OSICS Band C/AG with a range of 1528 nm to 1565 nm and the other was the Yenista OSICS AG L-Band with a range of 1568.7 nm to 1608 nm. In number 2 we have the same as in the previously test but now we need to consider the design of the PCB. In the PCB, as shown in Figure 4.11 for each photodiode we consider a biasing resistor of 10 $k\Omega$ making it possible to measure the current.

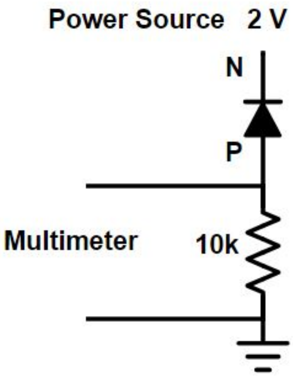

Figure 4.11: Photodiode implementation in PCB.

The power source used was the Tenma 75-10505 (number 4 in 4.10). The voltage measure was made using Keythley 2400-C and converted to current through the Ohm law:

$$I = \frac{V}{R} \tag{4.1}$$

To calculate the optical power so that we can compare it with the results from the first experiment it was used the following relation:

$$P(W) = \frac{I}{0.8} \tag{4.2}$$

$$P(dBm) = 10 \times \log(1000 \times P(W)) \tag{4.3}$$

The electrical output 1 results are presented in 4.12 and they are correlated with the output 2 of optical test (Figure 4.7).

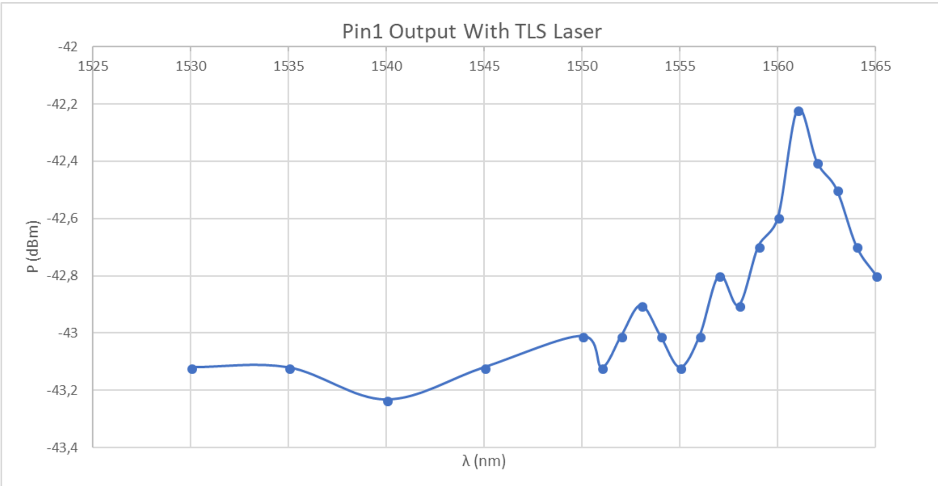

(a) TLS Laser in Input.

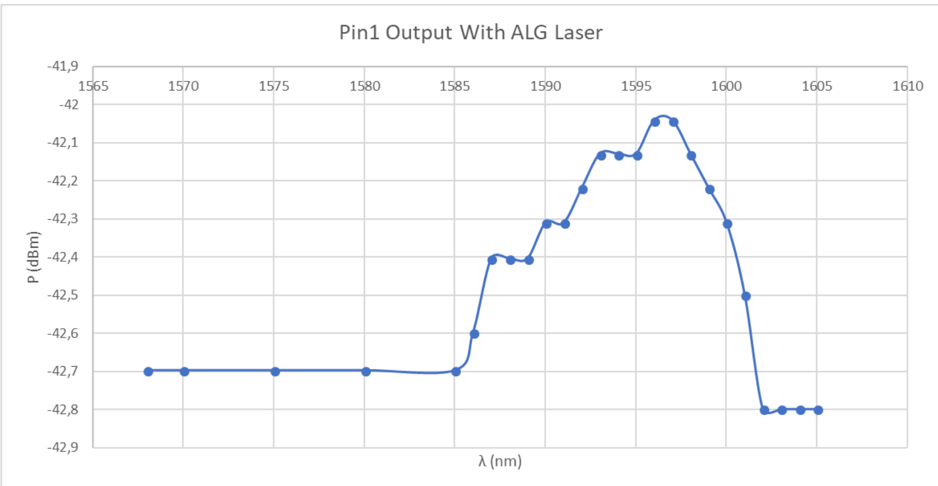

(b) AGL Laser in Input.

Figure 4.12: Optical power in output 1 as a function of wavelength.

As observed in Figure 4.12, the first eletrical output has a maximum in 1561 $\pm$ 0.1 nm with a repetition on 1596.5$\pm$0.1 nm. The FSR is 35.5$\pm$0.1 nm which compared to the optical results, has an error of 7.8%.

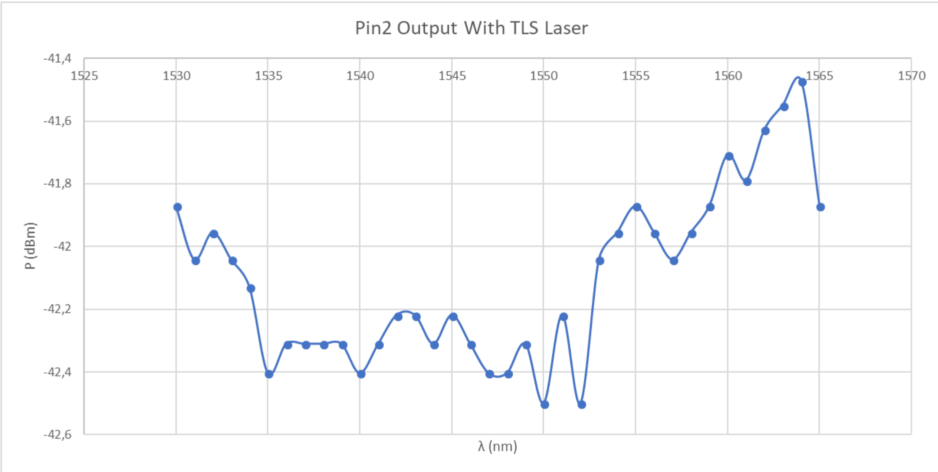

(a) TLS Laser in Input.

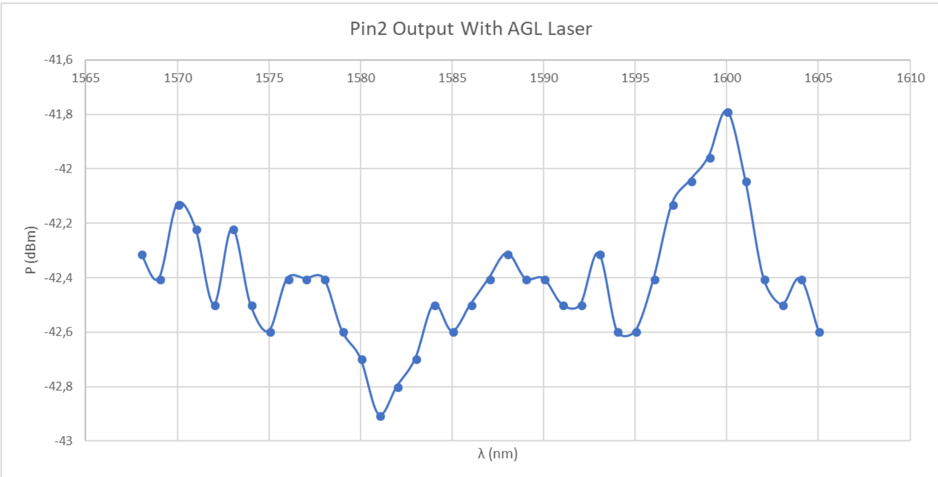

(b) AGL Laser in Input.

Figure 4.13: Optical power in output 2 as a function of wavelength.

Through the optical test, we can observe that the third electric output has a maximum near 1531 nm, 1569 nm and 1608 nm, and the first has near 1557 nm and 1596 nm. So the second electric output will have a maximum in the interval [1557 nm; 1569 nm] and in [1596 nm; 1608 nm]. In Figure 4.13, the second output has a maximum in 1564 $\pm$ 0.1 nm and 1600 ± 0.1 which corresponds to the previously predicted values. The FSR measure is 36 ± 0.1 nm which is close to the 38.5 nm with an error of 6.5%.

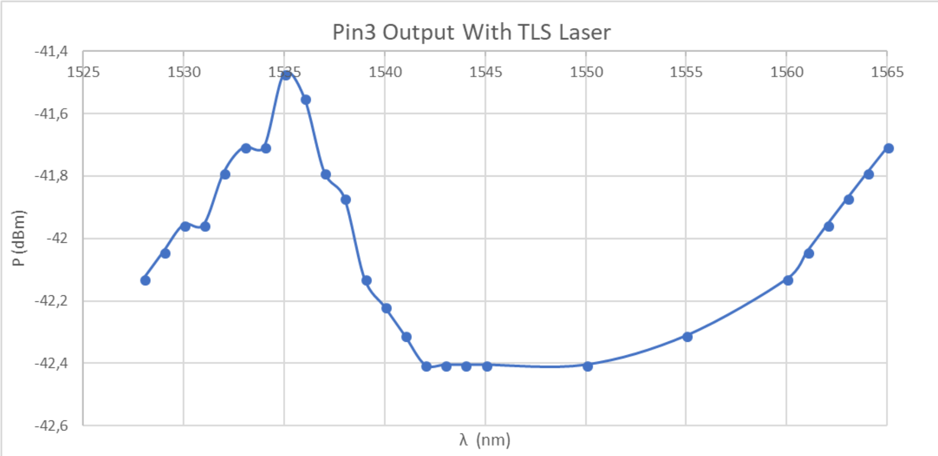

(a) TLS Laser in input.

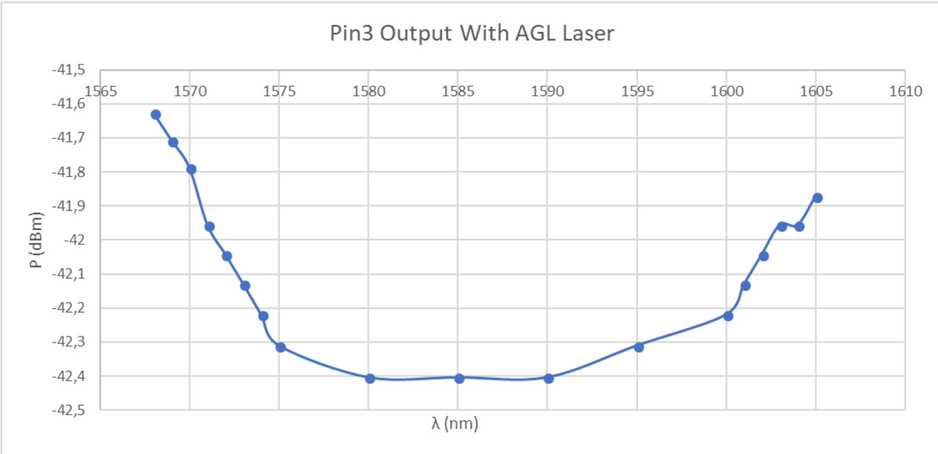

(b) AGL Laser in input.

Figure 4.14: Optical power in output 3 as a function of wavelength.

The third output has maximum points in 1535 ± 0.1 nm and 1535 ± 0.1 nm with a FSR of 31 ± 0.1 nm. These points have an error of 19.5% which is the least exact of the electrical outputs.

After completing the second test and observing the peak values of the figures, we can conclude that the maximum wavelength values are within the expected range but the power values are very low. The maximum optical power value (difference between the noise and the maximum peak) is 1 ± 0.1 dB. This was caused by the losses in PIC and because the optical alignment was not the best.

Similarly to the first section, the main difficulties were the fiber alignment and the reading of the values, in particular the power-meter since the voltage value was always changing. Another issue with the electrical test was the PCB design. The design used was the one presented in Figure 4.11 but it presents a major problem: the diode can stop conduction. This can occur when optical power increases the diode current and the voltage in the resistor also increases. Then, the PIN voltage will be lower than the threshold voltage and the diode can stop conducting. To overcome this problem instead of using a resistor in series with the PIN, we can use a model based on a current mirror.

4.3 Alignment Controller

As the final objective of this dissertation is the automation in PIC tests, one of the main problems that must be overcome, as seen previously, is the alignment of the optical fiber. In previous tests, even with Holders and V-Groove, which is already a breakthrough in automatic alignment, a lot of time is spent in alignment and any sudden movement in our setup can damage the alignment already done. In this section, an automatic optical alignment test will be demonstrated using the Thorlabs APT Modular Rack MMR602 controller which reduces the oscillations and instability associated to the user when controlling manually.

Thorlabs has an extensive range of one-, two- and three-axis controllers for stepper motor and piezo actuator control. The modular rack system provides a highly functional 12 channel platform within the 'footprint' of a 4U high, 19" wide enclosure, with a unified power supply and an USB communication interface [25].

The alignment is fast on the APT controller due to the fact that is done at the software level. The controller is shipped with a sophisticated multithreaded ActiveX based software control suite. This suite comprises the main ActiveX based APT Server with a number of utilities, including APTUser and APTConfig [25]. APT Server is the main software 'engine' that runs on the host PC to provide all necessary APT services such as generation of sophisticated graphical instrument panels, multiple USB communications units and multithreaded execution to enhance system operation and prevent GUI deadlock.

The APTUser application allows the user to interact with any of the connected modules. The program displays multiple graphical instrument panels to allow multiple APT modules to be controlled simultaneously. The APTConfig is used by the users who need to develop custom software. For the tests presented in this document the only software used was the APTUser and the module was the NanoTrak Control Module.

The APT Modular NanoTrak Controller is available for use with the Thorlabs APT Modular Motion Control System and represents the latest development in automated optical alignment technology [26]. It combines two channel piezoeletric controllers into a single plug-in unit with an intelligent active-feedback alignment control system. The architecture of the Nanotrak unit comprises a PIN photodiode and a transimpedance amplifier, a servo control loop and a dual channel HV amplifier output circuit for driving two piezo-actuators, connected to a positioning 3D-stage [26]. An example of the NanoTrak software is shown in Figure 4.15.

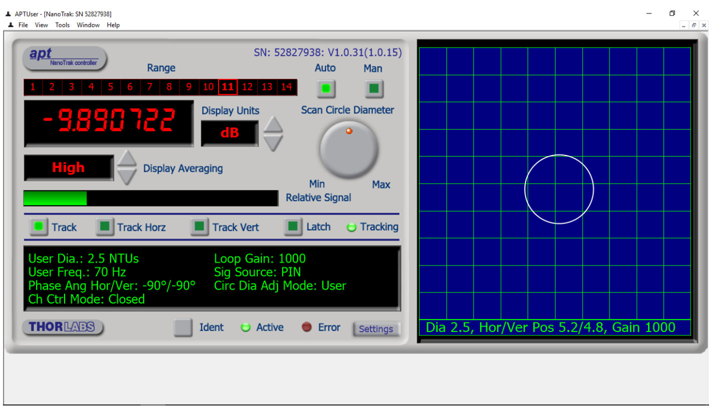

Figure 4.15: NanoTrak software GUI [26].

The test performed in this section is illustrated in Figure 4.16 and it aims to explain how to do automatic alignment using the APT Modular Rack and the NanoTrak module, which will be used in the final test.

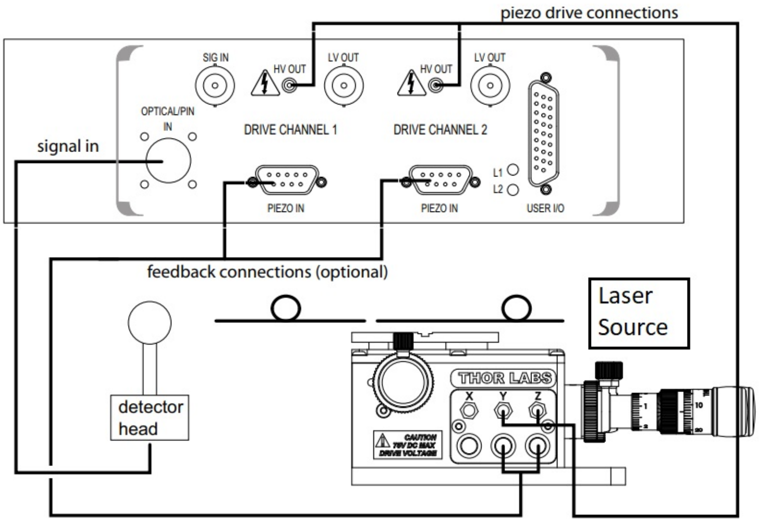

Figure 4.16: Example set up of the NanoTrak with the stage and optical fibers [26].

The steps for the automatic test are subsequently described [26]:

1. The connection was made from the 'HV OUT' terminals to the inputs of the stage, corresponding to horizontal and vertical motion;

2. The optical fibers, after well cleaved and clean, were placed in the stage, using a V-Groove holder, as represented in Figure 4.17.

3. Connect the fiber to the OPTICAL I/P. If using an external detector head, connect the output fiber to the detector head. If using the SMB-terminated cable, connect the detector head to the 'OPTICAL/PIN I/P' connector of the NanoTrak.

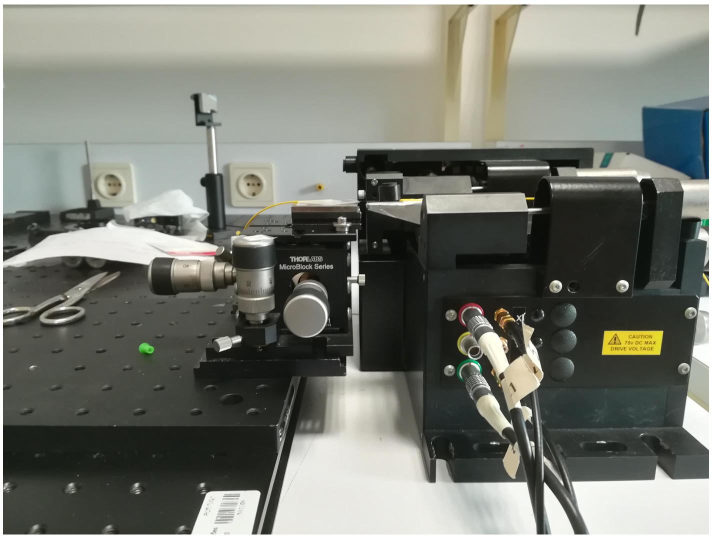

(a) The two stages.

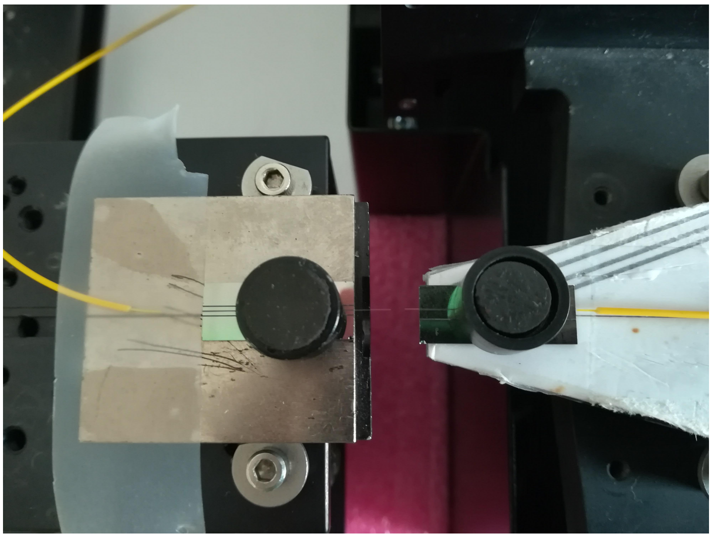

(b) The fiber alignment.

Figure 4.17: Test setup.

After connecting the cables it was necessary to follow the following steps in the NanoTrak Module available in APT User [26]:

1. Set the 'Scan Circle Diameter' control to approximately mid-position.

2. Press the 'Latch' button to select Latch mode and verify if the Latch indicator LED is lit.

3. Click and drag the scan circle in the display to the center.

4. Press the 'Auto' button to select 'Auto' mode. Ensure that the 'Auto' LED is lit.

5. Adjust the actuator on the positioning stage so that the fibers are well spaced apart, with zero power transmission between them. Make a note of the bar graph displays

of relative power input and range. Since the optical source has been removed, only background noise is registered (Figure 4.18).

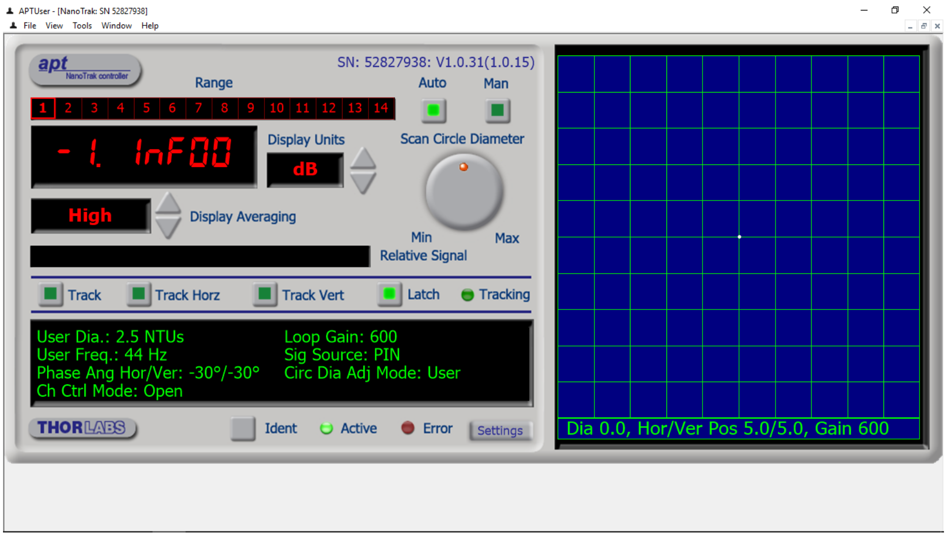

Figure 4.18: Background noise.

6. Use the actuators to bring the fiber tips together, until the display shows a significant increase indicating that the power has risen above the background level (Figure 4.19).

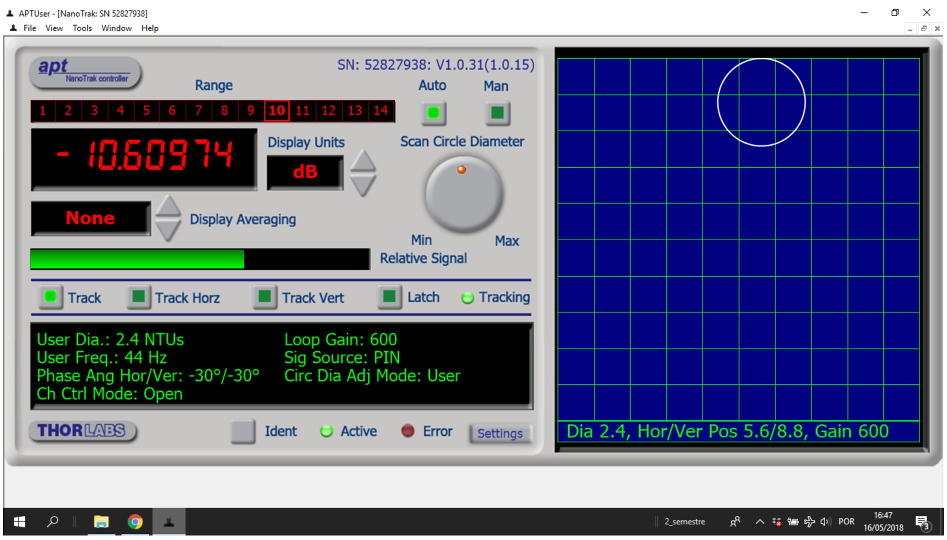

Figure 4.19: Significant optical power increase.

7. Press the 'Track' button to select Track mode. Verify if the 'Tracking' indicator is lit and that the circle moves towards the position of maximum power (center screen). The NanoTrak has now positioned the fiber to give the maximum optical power transmission.

If for any reason the circle on the screen reaches the edge of the display, it means that the piezo actuators cannot move far enough to reach the position of maximum power. The actuators must be manually adjusted to bring the circle away from the edge of the screen. If the circle tends to drift, increase the scan circle diameter and if the circle tends to oscillate, decrease the scan circle diameter [26]. The adjustments resume is shown in Figure 4.20.

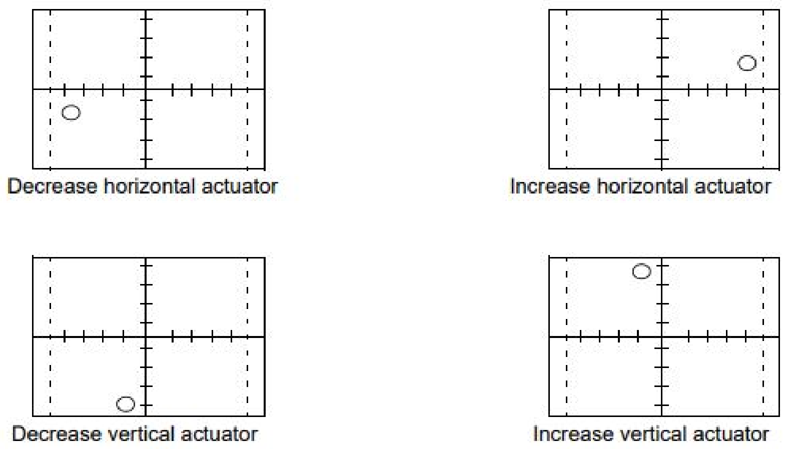

Figure 4.20: Actuator adjustments [26].

The maximum optical power received is illustrated in Figure 4.21 with an error of 0.1 dB. The input light source has 6.3 dBm power which means that it has 12 dB of loss associated.

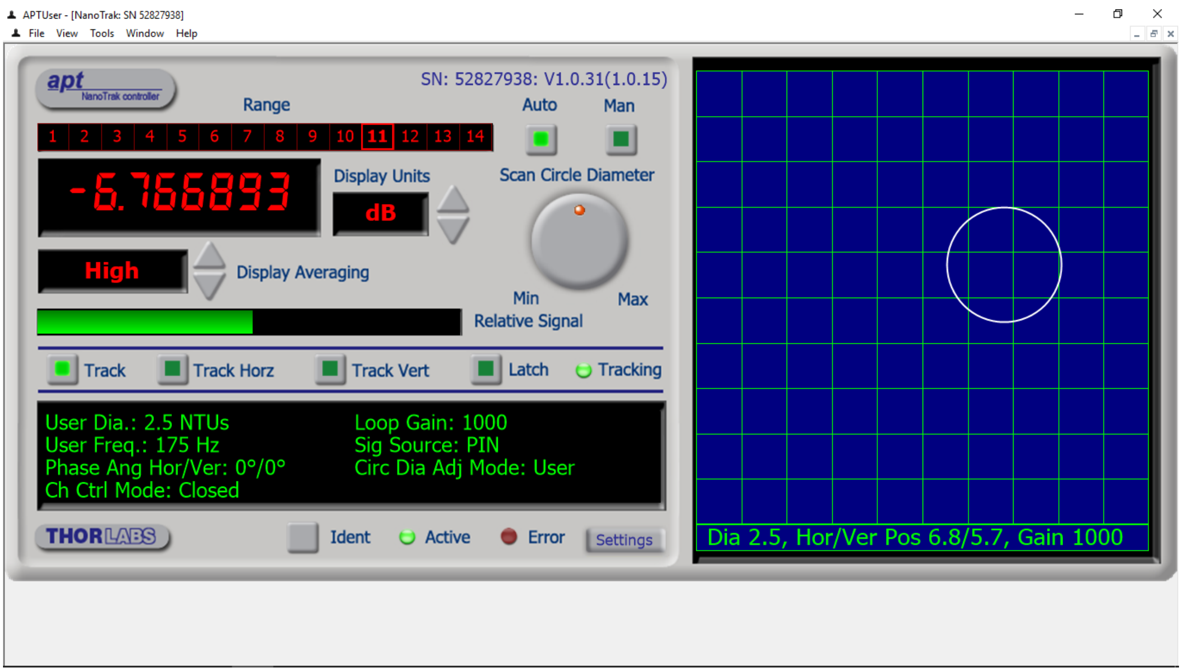

Figure 4.21: Maximum optical power received.

The main parameters that can be adjusted in alignment are:

- *Frequency* that consists in the frequency of the scanning circle. The frequency lies in the range of 15 to 200Hz and, if the frequency is 100Hz, it means that the stage makes 100 circular movements per second.

- *Loop Gain* that is the gain setting used to ensure that the DC level of the input signal lies within the dynamic range of the input. The loop gain value can be specified in the range of 100 to 10,000. As this value increases the more responsive is the behaviour of the NanoTrak.

- *Phase Compensations* that cancelled any phase shifts caused by electromechanical components. This parameter has 2 variables that separate the horizontal from the vertical component of the circle path. The values can be defined in the range -180 to 180 degrees and are set equal to each other.

- *Open Loop* or *Close Loop*. Commonly it is operated in Open Loop because the piezo amplifiers have a higher bandwidth operation. In closed-loop, position is maintained by a feedback signal from the piezo actuator strain gauge.

In conclusion, it was possible to perform an auto alignment in optical fiber allowing further use in the PIC testing. Some of the difficulties experienced in this test were the manual readjustment used to align the two fibers and the non linear relation of some of the parameters with the obtained results. One way to improve the alignment would be to use two NanoTraks, one in each stage.

4.4 Final Test - Total Automatization

After observing the difficulties of doing both an optical test and an electrical test in a PIC, this last test will have, as its final objective, the cancellation of the previous tests errors. In this experiment the optical alignment will be done using the APR Modular Rack MMR602 controller and the needed measures will be read directly through the personal computer, because now we will have a serial configuration, between all measuring instruments and our PC, through General Purpose Interface Bus (GPIB) cables controlled by Matlab code. To prove this concept, the reading of the first output of the optical test will be repeated. In this experience, we are not interested in the results, only in proving that it is possible to improve both the speed and the quality through the tests automatization.

Figure 4.22: Example of a GPIB cable.

The GPIB is a uniform interface that allows to connect and remotely control multiple test equipment, it is very flexible allowing data transfer between any connected instruments. When having a multiple connection, it is possible to have a bus or star configuration as shown in Figure 4.23.

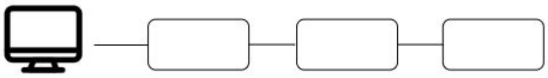

(a) Bus configuration.

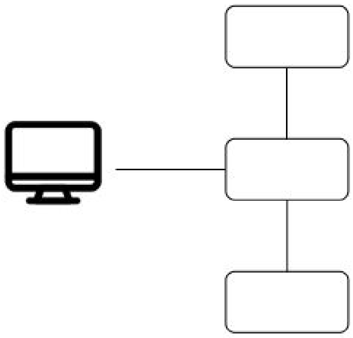

(b) Star configuration.

Figure 4.23: Type of configuration in a multiple connection.

Devices have a unique GPIB address on the bus and that address is allocated in the range of 0 to 30. This address allows each device to be distinguished from other devices. The maximum data rate achievable is always governed by the rate of the slowest device in the bus. When connecting multiple devices with a GPIB cable some cautions are required:

- Always disengage the instrument and the PC when connecting/disconnecting the communication cables;
- A maximum of 15 devices can be connected to the bus, along with the personal computer;
- Every device has its own address;
- To achieve maximum data transfer rates, the cable length should not exceed 20 meters total or an average of 2 meters per device;
- When carrying out communications, make sure that at least two-thirds of all connected devices are turned ON.

The Matlab supports GPIB communication through Instrument Control Toolbox. Once the data is transfered to MATLAB, it is possible to analyze and visualize the data coming from the instruments. There are two types of data that can be transferred over GPIB: instrument data and interface messages. The instrument data consists in specific commands that configure the devices and return measurement results. For a complete list of commands we needed to see the documentation for each device. The interface messages consist of commands that clear the GPIB bus, address devices, return self-test results, and so on [27]. The communication is established through a GPIB object, *gpib*, which is created in the MATLAB workspace. The process of communication concerning these steps follows an order: first we needed to create an interface object, connect it to the instrument and configure the values of baud rate in input and output data. After this, it is possible to write and read data, depending on the purpose of each test. In the end disconnect and clean up. The necessary commands for this steps can be found in [27].

The setup used in this test is shown in Figure 4.25, the only difference from the optical test setup is the addition of the APT Modular Rack MMR602 controller. All connections between the devices are in bus configuration as seen in Figure 4.24.

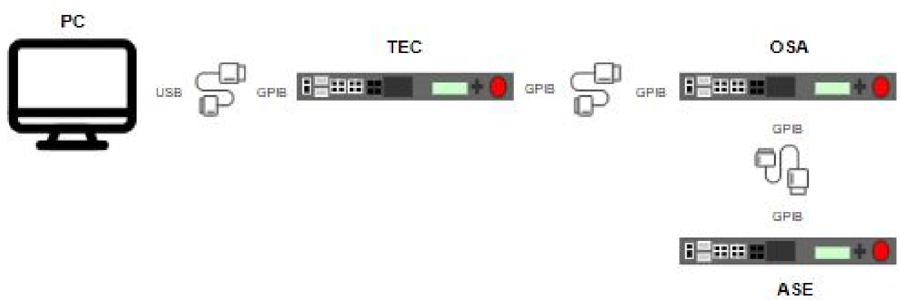

Figure 4.24: Bus configuration.

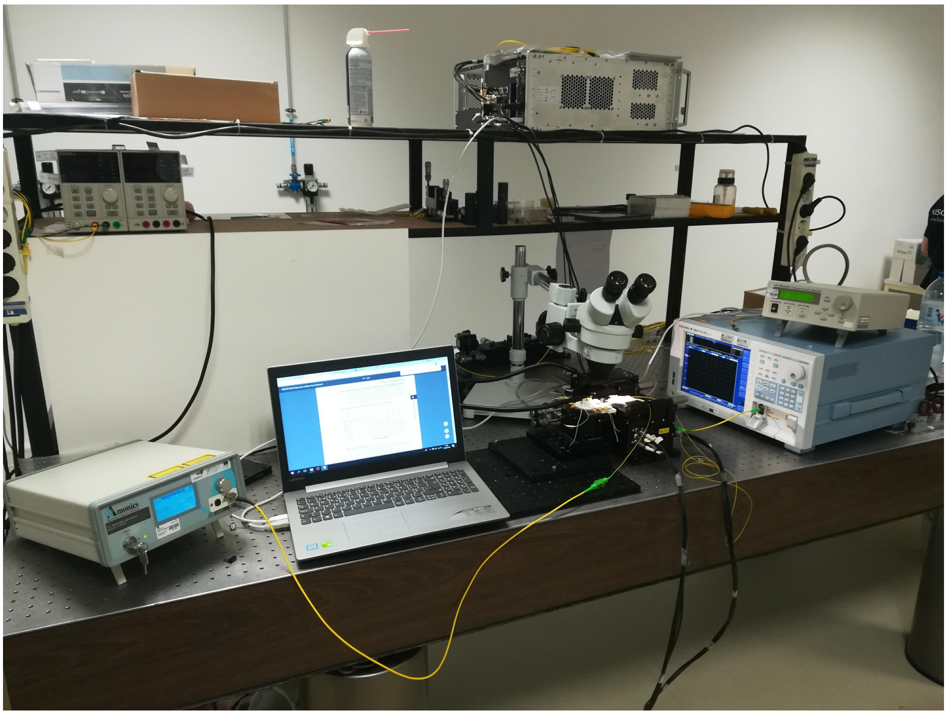

Figure 4.25: Automation test setup.

The maximum optical power received by the controller is shown in Figure 4.26 and the output 1 signal is shown in Figure 4.27. The code made in MATLAB followed the subsequent instructions:

- In the OSA read the values and create a graph with the input and output signals;

- In the ASE put the two channels in 335 mA and 500 mA respectively;

- In the TEC change the temperature of the PIC to $20°C$ and record the actual temperature.

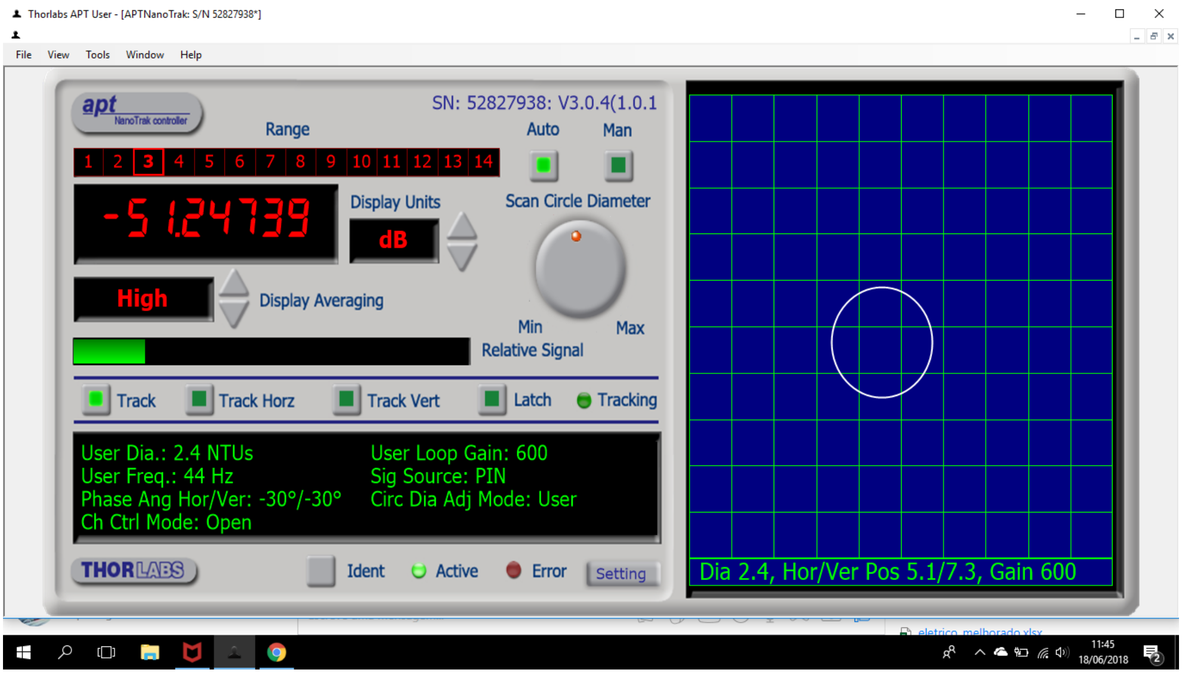

Figure 4.26: Auto alignment software.

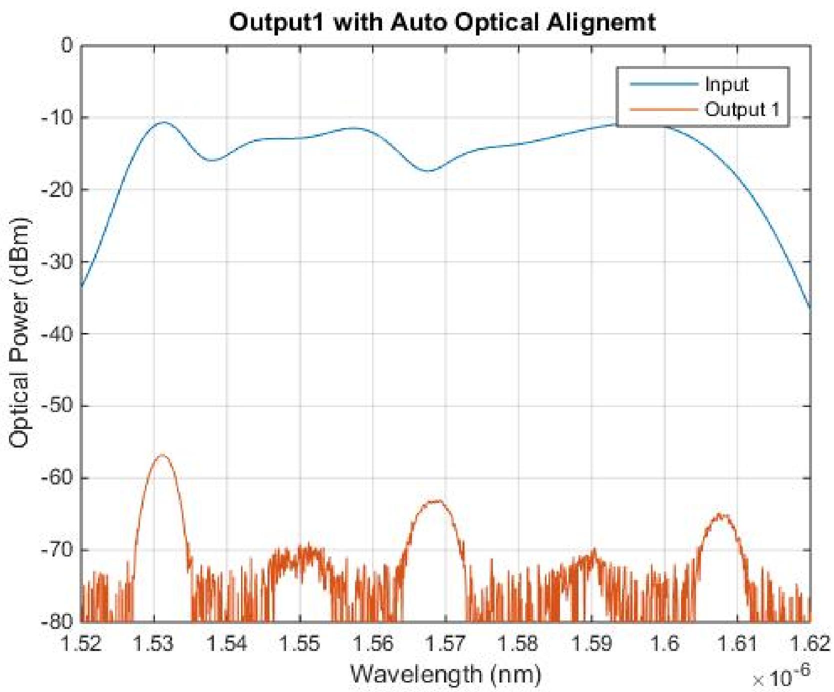

Figure 4.27: Final result.

At the end of the test, it is possible to conclude that using the controller for automatic alignment and having a multiple connection between the instruments with GPIB cables is quite advantageous. The first benefit is the easiness of the test performance and the improvement on the observation of the results. The second is the significant decrease of the test execution time .

It was expected that the optical power of output 1 would be higher, but it is still a valid value. This decrease in optical power may have occurred due to the changes in the laboratory environment. Another possible factor is that now the 3D stage has oscillation due to the frequency chosen by the user in the controller software that can interfere with the alignment. Another problem with this test was the communication with the ASE due to the lack of a manual with the control commands necessary to the MATLAB interface.

Chapter 5

Generic Testing Methodology

The realization of an experiment is a process that consumes a lot of time. What usually happens is to start the experiment and the data register without having done a prior preparation of the experience, such as not knowing the necessary assembly for its realization or the non-elaboration of the test procedure. The objective of this chapter is to create a test protocol to reduce the time spent in the laboratory and increase the accuracy of the tests in PICs.

In the first part of this chapter, and taking into account the previous section, it will be proposed a dedicated generic testbed for PICs characterization.

Finally, a PICs test procedure will be proposed, to facilitate and reduce the time spent in the laboratory.

5.1 Generic Test Setup

Test-bench suitable for generic PICs characterization is not yet present, in the laboratories, the only option possible is the manipulation of typical 3D stages [5]. The main problems in the PIC tests as seen before are the manual alignment and the organization and visualization of the data by the instruments. These factors affect the stability, the characterization and delay the measurements. As seen in the last chapter to overcome this problem it was used a stage with motorized control and a bus configuration of GPIB cables in a set of devices.

With the results obtained in the last chapter it is possible to think in a generic test setup to characterize a PIC in the shortest time possible. Figure 5.1 shows the proposed test setup block diagram. It consists of two main blocks each one connected to the personal computer of the researcher. One block consists of all measurement instruments and the connections between them. The other block aggregates the auto-alignment controller and the PIC montage.

Figure 5.1: Propose generic test setup.

The block named "Measurement Instruments" is shown in Figure 5.2. As shown if we have N devices are needed $N-1$ cables GPIB-GPIB and one cable USB-GPIB. In Section 4.4 we mentioned the concerns with the connection with GPIB cables. If the device chosen for the experiment does not have a GPIB input but has another remote control input (RS-232 or Ethernet) it is possible to make the connection using adapters.

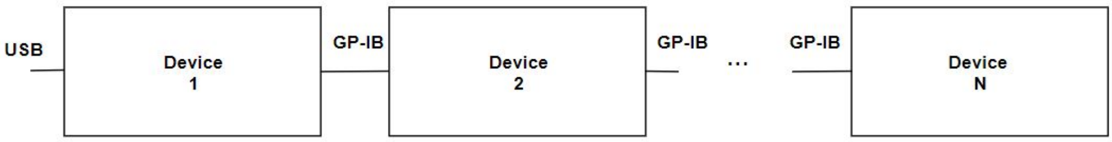

Figure 5.2: Measurement Instruments block.

The "Auto Alignment Controller + PIC Montage" is shown in Figure 5.3.

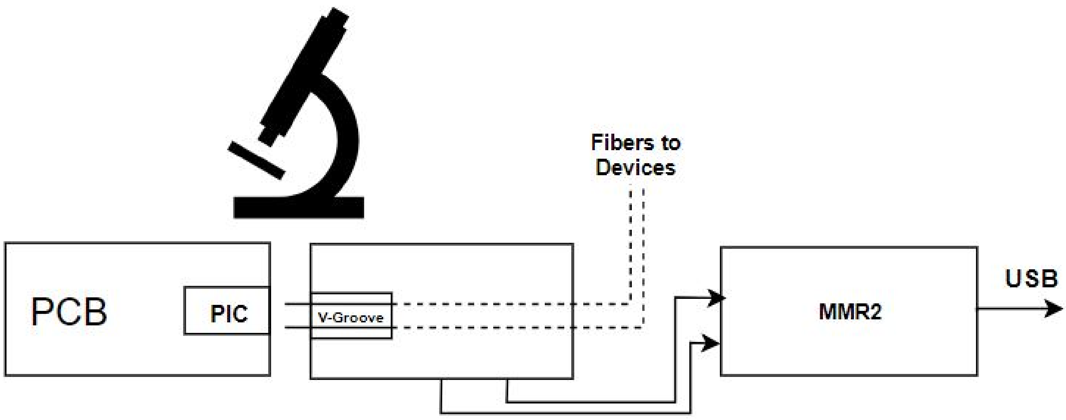

Figure 5.3: Auto Alignment Controller + PIC Montage block.

This block diagram can be separated into two parts. The first part is on the left side of Figure 5.3 and is composed by a fixed 3D stage that supports the PCB with the PIC inside. On the right side is represented a stage with motorized control to do the automatic alignment.

This stage supports the optical fibers that will be the optical inputs/outputs of the PIC, the V-Groove used depends on the number of optical fiber needed. The microscope between the PIC and the I/O fibers is used to make possible the visualization and control of the alignment.

This generic setup was proposed for speed-up, simplify the measurement procedure and the improvement of the measurement accuracy. With this setup is possible to have auto-alignment and to make the tests, both in the optical and electrical domains.

5.2 Test Protocol

For an experiment to be properly executed, it is necessary a previous preparation. The procedure of the experience is one of the most important factors for the success. In this section will be proposed a general procedure for a PIC test. Many steps of this procedure may seem simple but one of the objectives of this thesis is to show a complete procedure so that the researcher does not waste much time in the laboratory.

In the laboratory, the main materials for a PIC test are the measurement instruments and the 3D-stages that support the PIC and the optical fibers. Other materials required for a PIC testing are shown in Figure 5.4.

Figure 5.4: Materials required to a PIC test.

In Figure 5.4 [1] is shown a bottle of alcohol, plastic tweezers, allen wrench, fiber optics stripper, adhesive tape, leveling tool, optical fiber cleaver, air spray and clean paper.

The clean paper and the alcohol are used for the cleaning of both sides of the optical fiber and the air spray is for cleaning any dust in the PIC. The purpose of the allen wrench keys

[1]The description of the materials will be in the order of left right and down up.

kit and the leveling tool is for the 3D-Stage montage.

To manage the optical fiber first it is needed first to strip the fiber (remove the coating around the optical fiber) and cleave the fiber using an optical fiber cleaver. This fiber cleaver creates a perfectly flat end face, perpendicular to the longitudinal axis of the fiber allowing light transmission. Finally, the function of the adhesive tape and the plastic tweezers is to adjust the optical fiber and the V-groove in the stage.

Being described the general setup and all the materials needed for a PIC experience now it is possible to propose a test protocol. Next it is described the proposed test protocol based on the tests done previously and the observed constraints:

1. 3D-Stages assembly;
2. Connect the motorized stage with the controller and the controller with the PC via USB;
3. Setup all the measurement instruments and configure the bus/star connection between them via GPIB and connect the first device with the personal computer;
4. Optical fiber preparation: stripping, cleaving and cleaning;
5. Connect the optical fibers to the measurement instruments;
6. Optical auto-alignment though the software controller;
7. Start measurements;
8. Remote control of the devices and data organization via Matlab.

Following this protocol and using the generic test setup presented before it is possible to do a PIC testing with less difficulties than before, with more accurate results and the experience duration is significantly reduced.

Chapter 6

Conclusions and Future Work

6.1 Conclusions

The current trend of the telecommunications industry features a progressive demand for bandwidth from corporate and residential users that needs to be accompanied by an increase of the same magnitude for service providers. To achieved this the PON networks have evolved to improve the transmission capacity being the NG-PON2 the latest version of it.

The integrated optics represents an evolution in optical communications being possible to integrate various components in the same chip. The optical components can be separated into two groups, the active and passive. In Chapter 2 was only presented the AWG and the Photodetectors, because they composed the PIC available for the tests.

Chapter 3 addresses the measurement concept, the difference between the direct and indirect measurement and the error calculation in each case. This measurement theory is an important tool in experiments, necessary to evaluate the data and is used in all measures in this thesis.

To improve the accuracy and the time spent in PIC testing, first it was essential to understand the experiments difficulties. We started by testing a PIC in the optical and electrical domain with manual optical fiber alignment and data observed and recorded by the user. The PIC used divides the upstream and downstream in NG-PON2. In the optical domain, the results were as expected, apart from one of the outputs (output 2) that was degraded and unstable. It was caused by an imperfection in the waveguide making impossible a proper optical fiber alignment. In the electrical domain test, the results were as expected, however with higher losses compared to the first test.

The manual alignment and the data treatment were the difficulties observed in both tests. To overcome this two problems, first it was done an auto-alignment test using the Thorlabs APT Modular Rack controller. With the motorized stages it was possible to reduce the oscillations and instability introduced by the operator using manually controlled ones. The problem with the controller was the need of many manual adjustments, to make the final alignment possible, and the lack of documentation and information.

The last test solves the other problem, and it was done using a bus configuration between all measurement devices using GPIB cables. In this test we have total automation, being the alignment done with the controller, the devices controlled using MATLAB and the data received and processed by MATLAB. The advantages of the GPIB cables are the simple standard hardware interface, it is an interface present on many benches and it is possible to connect multiple instruments to a single controller.

The results were as expected, the decrease of the signal amplitude comparing to the first test could be caused by the exposure of the PIC in the laboratory and the output 1 as a failure in waveguide like output 2. With the tests complete it was possible to create a generic test setup and a protocol for PIC testing (Chapter 5). With it, it is possible to have better results with a drastic time reduction in tests.

Other error sources that could influence the results were the environmental changes in the laboratory. To overcome these problems a laboratory with controlled environment is needed.

6.2 Future Work

As the end of this work, the following topics may be interesting to proceed:

- Extend the study on the auto-alignment controller, searching for relations between the results and the parameters;
- Repeat the tests with two motorized stages controlled by the auto-alignment controller;
- Test other PICs composed by other components to prove that the generic test setup is validated for any PIC.

Bibliography

[1] Salem Bindhaiq, Abu Sahmah M Supa, Nadiatulhuda Zulkifli, Abu Bakar Mohammad, Redhwan Q Shaddad, Mohamed A Elmagzoub, Ahmad Faisal, et al. Recent development on time and wavelength-division multiplexed passive optical network (twdm-pon) for next-generation passive optical network stage 2 (ng-pon2). *Optical Switching and Networking*, 15:53–66, 2015.

[2] Govind P Agrawal. *Fiber-optic communication systems*, volume 222. John Wiley & Sons, 2012.

[3] Hélène Debrégeas-Sillard and Christophe Kazmierski. Challenges and advances of photonic integrated circuits. *Comptes Rendus Physique*, 9(9-10):1055–1066, 2008.

[4] John M Senior and M Yousif Jamro. *Optical fiber communications: principles and practice*. Pearson Education, 2009.

[5] E. Bitincka. *Generic testing in photonic IC's*. PhD thesis, TUE : Department of Electrical Engineering, 2015.

[6] Weicheng Xiong, Chanle Wu, Libing Wu, Xiaojun Guo, Yibo Chen, and Ming Xie. Ant colony optimization for pon network design. In *Communication Software and Networks (ICCSN), 2011 IEEE 3rd International Conference on*, pages 380–383. IEEE, 2011.

[7] Mohammad Azadeh. *Fiber optics engineering*. Springer, 2009.

[8] Ulrich Killat. *Access to B-ISDN via PONs: ATM communication in practice*. Springer Science & Business Media, 2012.

[9] The application of tdm-pon and wdm-pon. `http://www.fiber-optical-networking.com/the-application-of-tdm-pon-and-wdm-pon.html/winnt/kernel.htm`. Accessed: 2018-03-14.

[10] Cedric F Lam. *Passive optical networks: principles and practice*. Elsevier, 2011.

[11] Glen Kramer, Biswanath Mukherjee, and Ariel Maislos. Ethernet passive optical networks. *IP over WDM: Building the Next-Generation Optical Internet*, pages 229–275, 2003.

[12] CommScope. *GPON - EPON Comparison*. White Paper, October 2013.

[13] Ling Chen, Stefan Dahlfort, and Dave Hood. Evolution of pon: 10g-pon and wdm-pon. In *Communications and Photonics Conference and Exhibition (ACP), 2010 Asia*, pages 709–711. IEEE, 2010.

[14] Derek Nesset. Ng-pon2 technology and standards. *Journal of Lightwave Technology*, 33(5):1136–1143, 2015.

[15] Pan Pan, An Junming, Wang Liangliang, Wu Yuanda, Wang Yue, and Hu Xiongwei. Design and fabrication of an inp arrayed waveguide grating for monolithic pics. *Journal of Semiconductors*, 33(7):074010, 2012.

[16] RP Schneider, JL Pleumeekers, C Joyner, V Lal, AG Dentai, R Muthiah, D Lambert, S Hurtt, SW Corzine, S Murthy, et al. Inp-based photonic integrated circuits: Technology and manufacturing. In *Indium Phosphide & Related Materials, 2009. IPRM'09. IEEE International Conference on*, pages 334–338. IEEE, 2009.

[17] Radhakrishnan Nagarajan, Masaki Kato, Jacco Pleumeekers, Peter Evans, Scott Corzine, Sheila Hurtt, Andrew Dentai, Sanjeev Murthy, Mark Missey, Ranjani Muthiah, et al. Inp photonic integrated circuits. *IEEE Journal of selected topics in quantum electronics*, 16(5):1113–1125, 2010.

[18] Xaveer JM Leijtens, Berndt Kuhlow, and Meint K Smit. Arrayed waveguide gratings. In *Wavelength Filters in Fibre Optics*, pages 125–187. Springer, 2006.

[19] Salah Elfaki Elrofai. Review paper of array waveguide grating (awg). 2015.

[20] VPIPhotonics. *Introduction to Optical Receivers Rx1 - Lecture Series*. Univeristy Program Photonics Curriculum Version 8.0.

[21] Pedro Fonseca. Sistemas de instrumentação electrónica. *Universidade de Aveiro*, 12, 2011.

[22] Norman Charles Barford. *Experimental measurements: precision, error and truth*. Wiley, 1985.

[23] Philip R Bevington, D Keith Robinson, J Morris Blair, A John Mallinckrodt, and Susan McKay. Data reduction and error analysis for the physical sciences. *Computers in Physics*, 7(4):415–416, 1993.

[24] John R Taylor and ER Cohen. An introduction to error analysis: the study of uncertainties in physical measurements. *Measurement Science and Technology*, 9(6):1015, 1998.

[25] APT Modular Rack. `https://www.thorlabs.com/drawings/61ee448719f260b8-EB28DB8C-A00B-5E64-204C57ADA720BD77/MMR602-Manual.pdf`. Accessed: 2018-06-19.

[26] NanoTrak Control Module. `https://www.thorlabs.com/drawings/61ee448719f260b8-EB28DB8C-A00B-5E64-204C57ADA720BD77/MNA601_IR-Manual.pdf`. Accessed: 2018-06-19.

[27] MathWorks Support. `https://www.mathworks.com/support.html?s_tid=gn_supp`. Accessed: 2018-06-20.

Appendix A

Matlab *Software* for GPIB interface.

A.1 Total Automatization *Software*

```
%% Instrument Connection
clear all
clc

% Find a GPIB object, OSA.
obj2 = instrfind('Type', 'gpib', 'BoardIndex', 7, 'PrimaryAddress', 1, 'Tag',
'');

% Create the GPIB object if it does not exist
% otherwise use the object that was found.
if isempty(obj2)
    obj2 = gpib('AGILENT', 7, 1);
else
    fclose(obj2);
    obj2 = obj2(1);
end

% Find a GPIB object, TEC.
obj1 = instrfind('Type', 'gpib', 'BoardIndex', 7, 'PrimaryAddress', 4, 'Tag',
'');

% Create the GPIB object if it does not exist
% otherwise use the object that was found.
if isempty(obj1)
    obj1 = gpib('AGILENT', 7, 4);
else
    fclose(obj1);
    obj1 = obj1(1);
```

```
end

obj1.InputBufferSize = 2E5; %Specifies the total number of bytes that can be
%queued in the input buffer at one time.
obj1.OutputBufferSize = 2E5; % Specifies the total number of bytes that can be
%queued in the output buffer at one time.


obj2.InputBufferSize = 2E5;
obj2.OutputBufferSize = 2E5;

% Connect to instrument object, obj1.
fopen(obj1);
fopen(obj2);

%% Instrument Configuration and Control
idn = query(obj1, '*IDN?'); %
idn2 = query(obj2,'*IDN?');


fprintf(obj1,'TEC:T 15'); % TEC:T X Put the temperature for X (Ts)

t = query(obj1,'TEC:T?'); % read the temperature (T)
temperatura = str2num(t)


%Osa Span
fprintf(obj2,'SENSe:WAVelength:STARt 1520NM;STOP 1620NM ')

fprintf(obj2,'*TRG');

x_a = query(obj2, ':TRACE:X? TRA'); %x axis
y_a = query(obj2, ':TRACE:Y? TRA'); % y axis
xx_a = str2num(x_a);
yy_a = str2num(y_a);

x_b = query(obj2, ':TRACE:X? TRB');
y_b = query(obj2, ':TRACE:Y? TRB');

xx_b = str2num(x_b);
yy_b = str2num(y_b);

plot(xx_a,yy_a)
hold on
grid on
plot(xx_b,yy_b)
```

```
title('Output1 with Auto Optical Alignemt ')
xlabel('Wavelength (nm)')
ylabel('Optical Power (dBm)')
axis([1.52e-6 1.62e-6 -80 0])
h = legend('Input','Output 1')

%% Disconnect and Clean Up
% Disconnect all objects.
fclose(obj1);
fclose(obj2);

% Clean up all objects.
delete(obj1);
delete(obj2);

clear obj1;
clear obj2;
```